

ATLAS ANTIBODIES IN NEUROSCIENCE

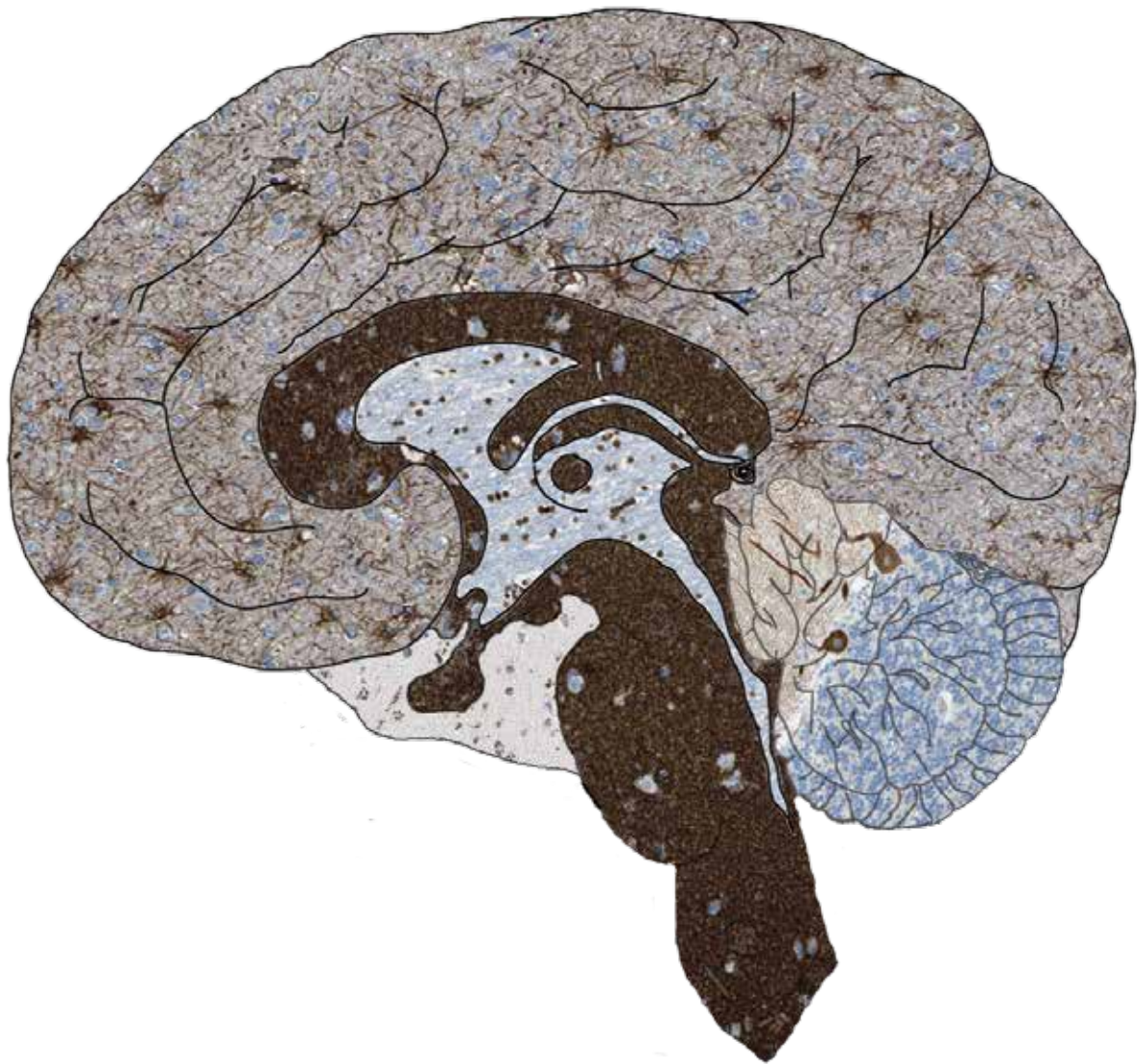


TABLE OF CONTENTS

Background - the Human Protein Atlas (4)



Triple A Polyclonals and PreciA Monoclonals (5)



Antibody Panel for Neuroscience (6-7)



Antibodies against proteins involved in Signaling (8-12)



Antibodies as Neural Lineage Markers (13-15)



**Antibodies against proteins involved in Aging and Neurodegenerative Disorders,
such as Alzheimer's, Parkinson's and Huntington's Diseases (16-17)**



Antibodies against proteins involved in Developmental Processes (18-19)



Antibodies on HPA Mouse Brain Atlas (20-22)



References (23)

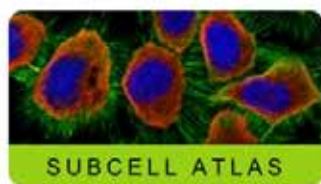


Contact (24)

THE HUMAN PROTEIN ATLAS



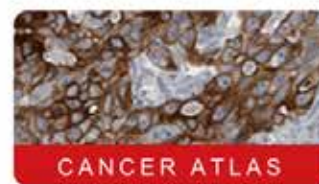
TISSUE ATLAS



SUBCELL ATLAS



CELL LINE ATLAS



CANCER ATLAS

SEARCH ? »

Search Fields »

e.g. insulin, PGR, CD36, or use Fields to search specific fields such as
protein_class:Transcription factors or chromosome:X

proteinalas.org

The Human Protein Atlas is Characterizing the Human Proteome

The Human Protein Atlas (HPA) project was initiated in 2003 by Swedish researchers, headed by Professor Mathias Uhlén, and funded by the Knut and Alice Wallenberg foundation^{1,2}. It is a unique world leading effort performing systematic exploration of the human proteome using antibodies.

The aim of the HPA project is to present an expression map of the complete human proteome. To accomplish this, highly specific Triple A polyclonal antibodies are developed to all protein coding human genes and protein profiling is established in a multitude of tissues and cells using tissue arrays. The antibodies are tested in immunohistochemistry (IHC), Western blot (WB) analysis, protein array assay and immunofluorescent based confocal microscopy (ICC-IF).

The Human Protein Atlas, October 2015

The 14th version of the Human Protein Atlas, released in April 2015, presents a tissue-based map of the complete human proteome. The extensive amount of data is divided into four separate 'sub atlases': the Tissue Atlas, the Cancer Atlas, the Subcell Atlas and the Cell Line Atlas. For all proteins represented in the Tissue Atlas, the expression profiles are based on IHC analysis on a large number of human tissues. The presentation of protein expression data in correlation to RNA sequencing data for each gene has now been included. In the Cancer Atlas, differentially expressed genes in several cancers can be studied, while the Subcell

Atlas presents subcellular localization by confocal microscopy. Additional information about protein expression in common cell lines is included in the Cell Line Atlas, which has become an appreciated toolbox for research.

Tissue microarrays containing samples from 44 different normal human tissues, 20 different cancer types and 44 different human cell lines are utilized within the project. The 44 normal tissues are present in triplicate samples and represent 82 different cell types. All normal tissue images have undergone pathology-based annotation of expression levels and are displayed on the normal Tissue Atlas presenting information regarding the expression profiles of human genes both on mRNA and protein level.

Validation in Human Neuro Tissues and Cell Lines

IHC images from human cerebellum, hippocampus, lateral ventricle wall and cerebral cortex tissues are available for the antibodies, as well as from stainings in the following brain cell lines: D341 Med, SH-SY5Y, U-138 MG, U-251 MG, U-87 MG. Malignant glioma tumor samples from up to 12 patients are presented for each antibody in the Cancer Atlas. In addition to IHC images, there are available immunofluorescence (ICC-IF) images from staining in U-251 MG cells for subcellular location information of the proteins.

HPA Mouse Brain Atlas

The protein atlas of the mouse brain project is a new addition to the Human Protein Atlas with the aim to increase the knowledge on protein expression and distribution in the mammalian brain. The basic architecture and organization of the

brain, sequence of functional domains within proteins and expression of genes are largely preserved throughout mammalian evolution. This enabled a successful expansion of the current data on protein expression in 4 brain regions (cerebral cortex, lateral ventricle, hippocampus and cerebellum) in the human to over 120 brain regions and subfields containing additional cell types in the much smaller mouse brain using the same antibodies raised against human proteins.

The first release of the HPA Mouse Brain Atlas contains protein expression profiles of 80 genes selected based on global expression (brain vs. peripheral organs), differential expression in the brain (brain regions), cellular expression (neurons, glia and others) and function (physiology, development or disease).



References:

1. Uhlén M *et al.* (2010) Towards a knowledge-based Human Protein Atlas. *Nat Biotechnol* 28(12):1248-50.
2. Uhlén *et al.* (2015) Proteomics. Tissue-based map of the human proteome. *Science* 23;347(6220).

Triple A Polyclonals

Triple A Polyclonals - the Building Blocks of HPA

The uniqueness and low cross reactivity of Triple A Polyclonals to other proteins are due to a thorough selection of antigen regions, affinity purification on the recombinant antigen, validation using several methods and a stringent approval process.

Development

The Triple A Polyclonals are developed against recombinant human Protein Epitope Signature Tags (PrESTs) of approximately 50 to 150 amino acids. These protein fragments are designed, using a proprietary software, to contain unique epitopes present in the native protein suitable for triggering the generation of antibodies of high specificity. This is achieved by a complete human genome scanning to ensure that PrESTs with the lowest ho-

mology to other human proteins are used as antigens.

Approval

The approval of the Triple A Polyclonals relies on a combined validation of the experimental results using IHC, WB or ICC-IF, from RNA sequencing and from information obtained via bioinformatics prediction methods and literature. Since the literature is often inconclusive, an important objective of the HPA project has been to generate paired antibodies with non-overlapping epitopes towards the same protein target, allowing the results and validation of one antibody to be used to validate the other one.

Triple A Polyclonal catalog

Today, there are more than 18,000 Triple A Polyclonals and new antibodies are added each year.

The antibodies developed and characterized within the Human Protein Atlas project are made available to the scientific community by Atlas Antibodies under the brand name Triple A Polyclonals.



PrecisA Monoclonals

Atlas Antibodies also provide a selected number of mouse monoclonal antibodies, under the brand name PrecisA Monoclonals. The PrecisA Monoclonals catalog is regularly expanding with new products every year.

Unique Features

Special care is taken in offering clones recognizing only unique non-overlapping epitopes and/or isotypes. Using the same stringent PrEST production process and characterization procedure as for the Triple A Polyclonals, the PrecisA Monoclonals offer outstanding performance in approved applications, together with defined specificity, secured continuity and stable supply. In general they also permit high working dilutions and contribute to more standardized assay procedures.

Clone Selection

Functional characterization is performed on a large number of ELISA positive cell supernatants to select the optimal clones for each application prior to subcloning and expansion of selected hybridomas.

Epitope Mapping

Clones are epitope-mapped using synthetic overlapping peptides in a bead-

based array format for selection of clones with non-overlapping epitopes only.

Isotyping

All PrecisA Monoclonals antibodies are isotyped to allow for multiplexing using isotype-specific secondary antibodies.

Hybridoma Cell Cultivation

Atlas Antibodies use in-vitro methods for the production scale-up phase thus replacing the use of mice for production of ascites fluid.

Antibody Characterization

The characterization of PrecisA Monoclonals starts with an extensive literature search to select the most relevant and clinically significant tissues to use for IHC characterization. Often there are more than one tissue type displayed in the IHC application data for each antibody. In addition to positive stained tissue, a negative control tissue staining is also displayed and if relevant, clinical cancer tissue staining.

The Western blot (WB) characterization includes results from endogenous human cell or tissue protein lysates or optionally

recombinant full-length human protein lysates.

Each PrecisA Monoclonal is thus supplied with the most relevant characterization data for its specific target.

PrecisA Monoclonals are developed by Atlas Antibodies, based on the knowledge from the Human Protein Atlas with careful antigen design and extended validation of antibody performance. With precise epitope information following all monoclonals, these precise, accurate and targeted antibodies are denoted PrecisA Monoclonals.



The product numbers of Triple A Polyclonals start with "HPA" and of PrecisA Monoclonals with "AMAb".

NEUROSCIENCE MARKER PANEL

The newly developed neuroscience marker panel consists of Precisa Monoclonals antibodies designed to recognize the main anatomical and neurochemical cell types in rodent and human nervous system.

We have taken great care to be able to offer these markers as tools for mapping the structures and cell types in the central and peripheral nervous system.

- Selected target proteins are expressed only by a single cell type
- IHC-validation in rat, mouse and human tissues
- WB-validation in mouse and human tissue lysates for the majority of the markers
- Antibodies of different isotypes, allowing for multiplexing experiments

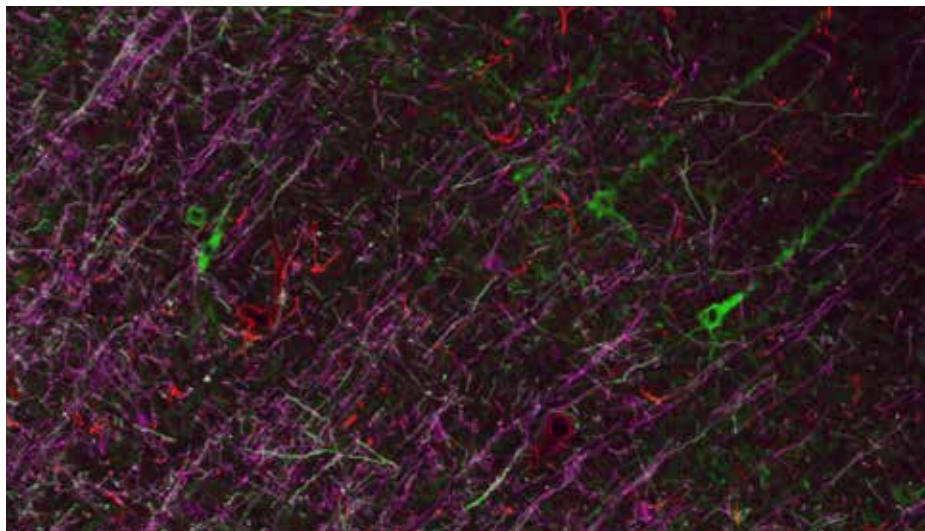


Figure 1.

Multiplexed IHC-IF staining of a coronal section of rat brain visualizing neurons in green, oligodendrocytes in magenta and astrocytes in red. Anti-NEFM antibody of isotype IgG2b (AMAb91030) is used to show neurons and their processes, oligodendrocytes are detected by Anti-CNP antibody of isotype IgG2a (AMAb91068) and astrocytes by Anti-GFAP antibody of isotype IgG1 (AMAb91033).

Markers for Neural Lineage and Signaling

The Neuroscience Marker panel consists of 34 antibodies targeting neural lineage markers and signaling markers. The panel includes neural lineage markers for neurons, astrocytes and oligodendrocytes/Schwann cells. Signaling markers target the glutamate, GABA, acetylcholine, noradrenaline, dopamine and serotonin systems.

Figure 1 shows coronal section of rat brain labeled with markers for three different cell

and astrocytes. The antibodies used are Anti-NEFM (AMAb91030), Anti-CNP (AMAb91068) and Anti-GFAP (AMAb91033) respectively.

In Figure 2, some of the major brain neurotransmitter systems are shown on sagittal mouse brain section. The image demonstrates the GABAergic system, glutamatergic system and acetylcholine system, here visualized by the Anti-GAD1 (AMAb91076), Anti-VGLUT1 (AMAb91041) and Anti-CHAT (AMAb91129) antibodies respectively.

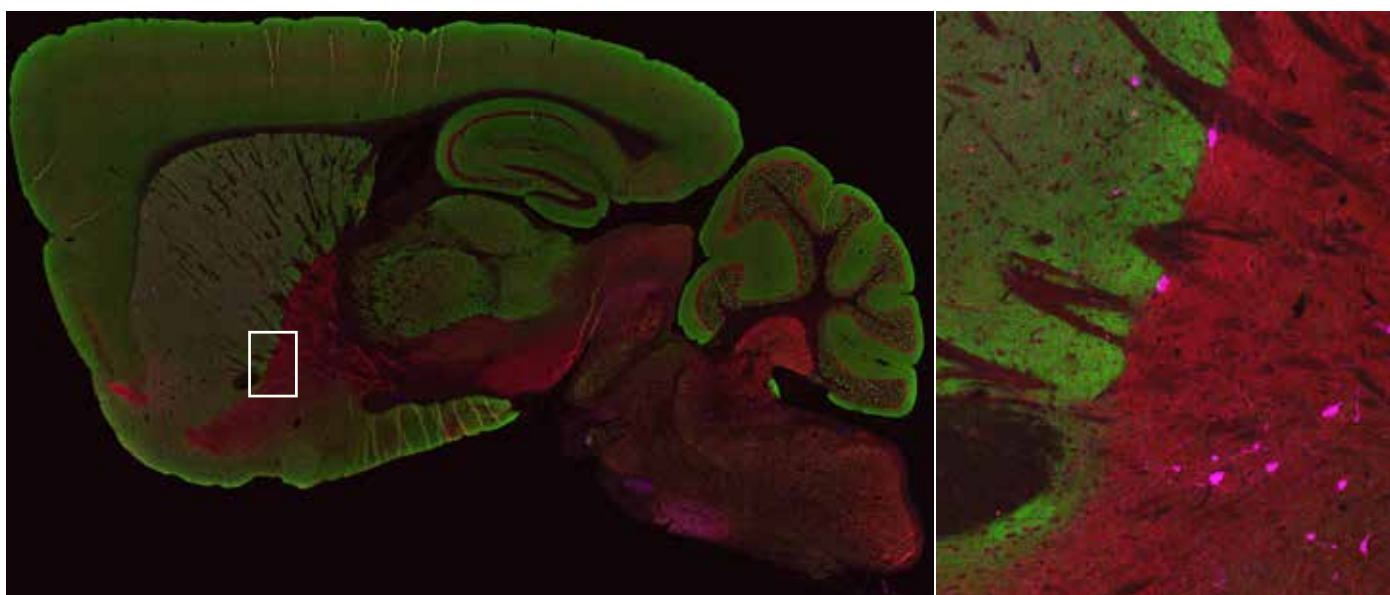


Figure 2.

Left: Multiplexed IHC-IF staining of sagittal mouse brain section showing the GABAergic system in red, glutamatergic system in green and acetylcholine system in magenta. The Anti-GAD1 antibody of isotype IgG2a (AMAb91076) is used as marker for the GABAergic system, Anti-VGLUT1 antibody of isotype IgG2b (AMAb91041) for the glutamatergic system and Anti-CHAT antibody of isotype IgG1 (AMAb91129) is used to visualize the acetylcholine system. Right: High-power image demonstrates the three systems in the basal forebrain (caudate putamen/globus pallidus), using the same antibodies.

High Specificity and Interspecies Reactivity

PrecisA Monoclonals Neuroscience markers show high specificity and selectivity for their target proteins. On the right, there is an example of the Anti-NET (AMAb91116) monoclonal antibody. This antibody recognizes the norepinephrine/noradrenaline transporter (NET, SLC6A2) and can be used to detect both noradrenergic cell bodies and processes in rat, mouse and human nervous system. The Anti-NET antibody AMAb91116 is highly-specific and does not show any cross-reactivity with e.g. dopamine transporter (SLC6A3, DAT).

Figure 3 shows specific staining of noradrenergic cell bodies and fibers in rat locus coeruleus (A), noradrenergic fibers in mouse cerebral cortex (B) and noradrenergic cell bodies and fibers in human locus coeruleus (C). The specificity of the AMAb91116 is further demonstrated on image D. It shows a coronal section of rat brain at the level of caudate putamen stained with Anti-NET (AMAb91116) in green and Anti-DAT (AMAb91125) in magenta. The caudate putamen is virtually devoid of noradrenaline fibers, only single ones can sometimes be observed (in green), while a dense network of thin dopamine fibers is seen in caudate putamen (in magenta).

Table 1.

Description of the PrecisA Monoclonals Neuroscience Markers.

| Marker for | Product Name | Product Number | Validated Applications | Isotype |
|---------------------------------|-----------------------|----------------|------------------------|---------|
| Neurons | Anti-NEFM (NF160) | AMAb91027 | IHC*, WB* | IgG1 K |
| Neurons | Anti-NEFM (NF160) | AMAb91028 | IHC*, WB* | IgG1 K |
| Neurons | Anti-NEFM (NF160) | AMAb91029 | IHC*, WB* | IgG2a K |
| Neurons | Anti-NEFM (NF160) | AMAb91030 | IHC*, WB* | IgG2b K |
| Neurons | Anti-NEFH (NF200) | AMAb91025 | IHC, WB | IgG1 K |
| Neurons | Anti-UCHL1 (PGP9.5) | AMAb91145 | IHC*, WB* | IgG1 |
| Astrocytes | Anti-GFAP | AMAb91033 | IHC*, WB* | IgG1 K |
| Astrocytes | Anti-S100B | AMAb91038 | IHC*, WB | IgG1 K |
| Astrocytes | Anti-GLUL | AMAb91101 | IHC*, WB* | IgG1 |
| Astrocytes | Anti-GLUL | AMAb91102 | IHC*, WB* | IgG1 |
| Astrocytes | Anti-GLUL | AMAb91103 | IHC*, WB* | IgG2a K |
| Schwann cells, oligodendrocytes | Anti-MBP | AMAb91062 | IHC*, WB* | IgG2a K |
| Schwann cells, oligodendrocytes | Anti-MBP | AMAb91063 | IHC*, WB* | IgG1 |
| Schwann cells, oligodendrocytes | Anti-MBP | AMAb91064 | IHC*, WB* | IgG1 |
| Oligodendrocytes | Anti-MOG | AMAb91066 | IHC*, WB | IgG1 |
| Oligodendrocytes | Anti-MOG | AMAb91067 | IHC*, WB | IgG1 |
| Oligodendrocytes | Anti-CNP | AMAb91068 | IHC*, WB* | IgG2a K |
| Oligodendrocytes | Anti-CNP | AMAb91069 | IHC*, WB* | IgG1 |
| Oligodendrocytes | Anti-CNP | AMAb91072 | IHC*, WB* | IgG2b K |
| Acetylcholine neurons | Anti-CHAT | AMAb91130 | IHC* | IgG2b |
| Acetylcholine neurons | Anti-CHAT | AMAb91129 | IHC* | IgG1 |
| Glutamate neurons | Anti-SLC17A7 (VGLUT1) | AMAb91041 | IHC*, WB | IgG2b K |
| Glutamate neurons | Anti-SLC17A6 (VGLUT2) | AMAb91081 | IHC* | IgG1 |
| Glutamate neurons | Anti-SLC17A6 (VGLUT2) | AMAb91086 | IHC* | IgG1 |
| GABA neurons | Anti-SLC32A1 (VGAT) | AMAb91043 | IHC* | IgG1 λ |
| GABA neurons | Anti-GAD1 (GAD67) | AMAb91076 | IHC*, WB | IgG2a K |
| GABA neurons | Anti-GAD1 (GAD67) | AMAb91078 | IHC*, WB | IgG1 |
| GABA neurons | Anti-GAD1 (GAD67) | AMAb91079 | IHC*, WB* | IgG2b K |
| GABA neurons | Anti-GAD2 (GAD65) | AMAb91048 | IHC*, WB* | IgG1 K |
| Dopamine neurons | Anti-SLC6A3 (DAT) | AMAb91125 | IHC* | IgG1 |
| Dopamine neurons | Anti-DDC | AMAb91089 | IHC*, WB | IgG1 |
| Noradrenaline neurons | Anti-SLC6A2 (NET) | AMAb91116 | IHC* | IgG1 |
| Dopamine and noradrenaline | Anti-TH | AMAb91112 | IHC* | IgG1 |
| Serotonin neurons | Anti-TPH2 | AMAb91108 | IHC* | IgG1 |

* Validated for human and rodent samples

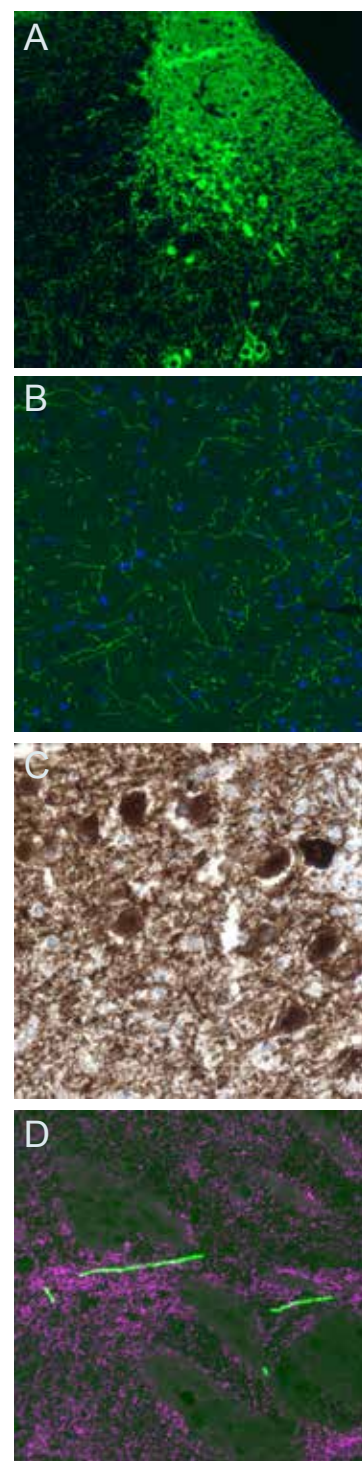


Figure 3.

IHC-IF (A, B, D) and bright-field (C) IHC staining demonstrating specificity and selectivity of Anti-NET antibody (AMAb91116) in rat (A, D), mouse (B) and human (C) brain. Staining with Anti-NET (AMAb91116) is shown in green (A, B, D) and in brown (C). DAT immunoreactivity is visualized in magenta using Anti-DAT antibody (AMAb91125).

SIGNALING

| Product Name | Product Number | Applications | Antigen seq identity to mouse / rat |
|----------------------------|--------------------------|----------------|-------------------------------------|
| Anti-ATF2 | HPA022134 | IHC,WB*,ICC-IF | 99 / 99% |
| Anti-ATF3 | AMAb90909 | IHC | 92 / 92% |
| Anti-ATF3 | HPA001562 ¹⁻³ | IHC,WB*,ICC-IF | 92 / 92% |
| Anti-ATP1B1 | HPA012911 | IHC,WB | 93 / 93% |
| Anti-ATP1B2 | HPA010698 | IHC | 96 / 88% |
| Anti-CAMK2B | HPA026307 | IHC,WB* | 96 / 96% |
| Anti-CAMK2D | HPA026281 | IHC | 100 / 97% |
| Anti-C-FOS | HPA018531 ⁴ | IHC,WB*,ICC-IF | 94 / 94% |
| Anti-CHAT | AMAb91130 | IHC | 96 / 96% |
| Anti-CHAT | HPA048547 | IHC | 96 / 96% |
| Anti-CHRM1 (M1 mAChR) | HPA014101 | IHC | 98 / 97% |
| Anti-CHRM2 (M2 AChR) | HPA029795 | IHC | 88 / 86% |
| Anti-CHRNA7 (alpha7 nAChR) | HPA029422 | IHC,WB | 98 / 95% |
| Anti-CLIC4 | HPA008019 ^{5,6} | IHC,WB,ICC-IF | 98 / 97% |
| Anti-CREB1 | HPA019150 | IHC,WB*,ICC-IF | 100 / 100% |

* WB both in human and rodent samples

1. Wu X *et al.* Opposing roles for calcineurin and ATF3 in squamous skin cancer. *Nature* 2010 May 20;465(7296):368-72.

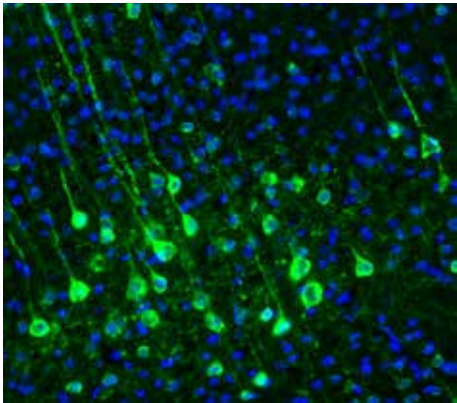
2. Hai T *et al.* Immunohistochemical Detection of Activating Transcription Factor 3, a Hub of the Cellular Adaptive-Response Network. *Methods Enzymol* 2011; 490:175-194.

3. Wei S *et al.* The Activating Transcription Factor 3 Protein Suppresses the Oncogenic Function of Mutant p53 Proteins *J Biol Chem* 2014/03/28 289(13):8947-8959. Epub 2014/02/19.

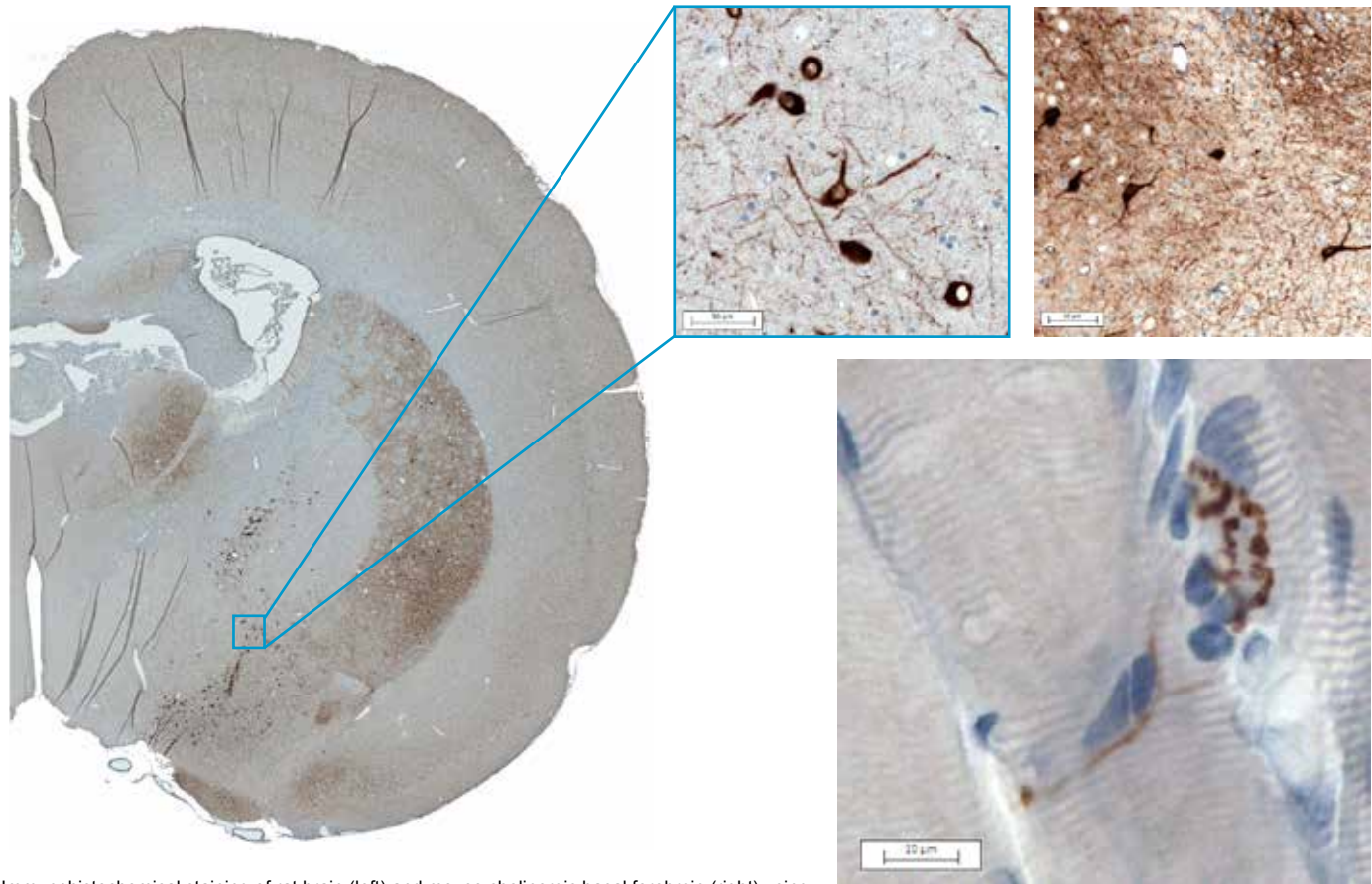
4. Pio R *et al.* Early Growth Response 3 (Egr3) Is Highly Over-Expressed in Non-Relapsing Prostate Cancer but Not in Relapsing Prostate Cancer. *PLoS One* 2013 28(1):e54096.

5. Lomnyska Ml *et al.* Impact of genomic stability on protein expression in endometrioid endometrial cancer *Br J Cancer* 2012 Mar 27; 106(7):1297-1305. Epub 2012/03/13.

6. Yan H *et al.* Histamine H3 receptors aggravate cerebral ischaemic injury by histamine-independent mechanisms. *Nat Commun* 2014 253334. Epub 2014/02/25.



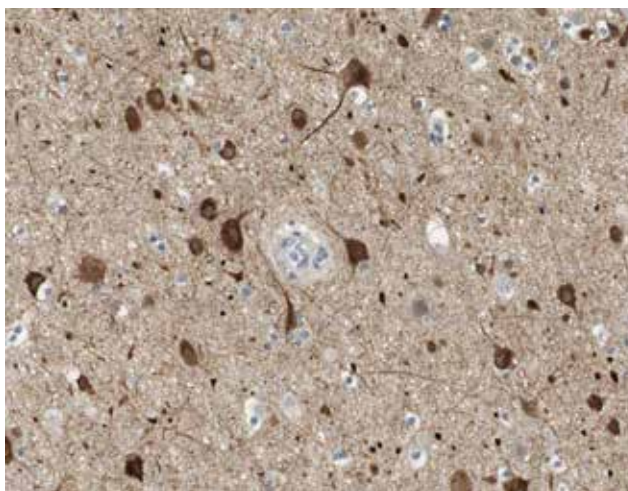
Calmodulin-dependent protein kinase II beta is expressed in various neuron populations in the mouse brain including pyramidal neurons in the somatosensory cortex. This is illustrated using the Anti-CAMK2B antibody (HPA026307).



Immunohistochemical staining of rat brain (left) and mouse cholinergic basal forebrain (right) using Anti-CHAT antibody (HPA048547) shows strong immunoreactivity in cholinergic cell bodies and terminals. High power image in the lower right corner demonstrates ChAT immunoreactivity in the motor end-plates in rat skeletal muscle. ChAT=choline O-acetyltransferase, enzyme catalyzing biosynthesis of acetylcholin.

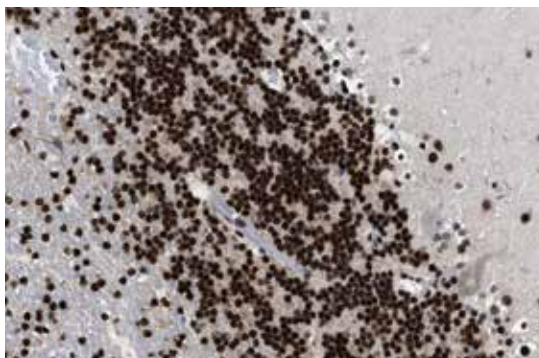
| Product Name | Product Number | Applications (human tissues) | Antigen seq identity to mouse / rat |
|--------------------------|--------------------------|------------------------------|-------------------------------------|
| Anti-DAT | HPA013602 | IHC,WB | 85 / 85% |
| Anti-DDC | AMAb91089 | IHC,WB | 90 / 88% |
| Anti-DDC | HPA017742 | IHC,WB*,ICC-IF | 90 / 88% |
| Anti-EAAC1 | HPA020086 | IHC | 77 / 79% |
| Anti-EAAT2 | HPA009172 | IHC | 87 / 89% |
| Anti-GABRA3 | HPA000839 | IHC,WB* | 91 / 93% |
| Anti-GABRB1 | HPA051297 | IHC | 97 / 100% |
| Anti-GABRG1 | HPA035622 ⁷ | IHC | 96 / 94% |
| Anti-GAD1 (GAD67) | AMAb91076 | IHC,WB | |
| Anti-GAD1 | HPA058412 | IHC,WB | 94 / 94% |
| Anti-GAD2 | AMAb91048 | IHC,WB* | |
| Anti-GAD2 | HPA044637 | IHC | 84 / 88% |
| Anti-GAT1 | HPA013341 | IHC,WB* | 98 / 98% |
| Anti-GAT3 | HPA037981 | IHC,WB | 85 / 87% |
| Anti-GLUR2 (AMPA2) | HPA008441 ^{8,9} | IHC | 100 / 100% |
| Anti-HTR2A | HPA014011 | IHC | 95 / 97% |
| Anti-KCC4 | HPA041652 | IHC,WB* | 84 / 82% |
| Anti-KCNJ5 (KIR3.4) | HPA017353 ¹⁰ | IHC,WB | 89 / 89% |
| Anti-KCNN2 (KCA2.2) | HPA038221 | IHC | 96 / 97% |
| Anti-KIF11 ¹¹ | HPA010568 | IHC,WB*,ICC-IF | 88 / 83% |

* WB both in human and rodent samples

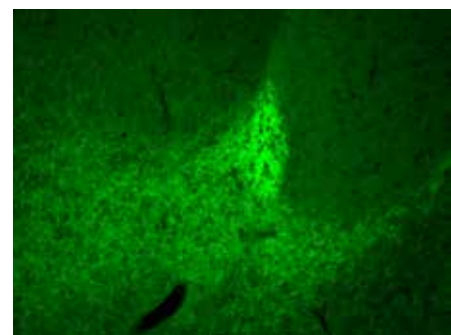


The Anti-MGLUR1 antibody (HPA015701) against glutamate receptor, metabotropic 1 strongly labels cortical perikarya, shown by IHC in human cerebral cortex tissue.

The cAMP responsive element binding protein 1 is strongly expressed in the granular layer of the cerebellum and in human neuronal glioblastoma U251 cells. This is illustrated using the Anti-CREB1 antibody (HPA019150).



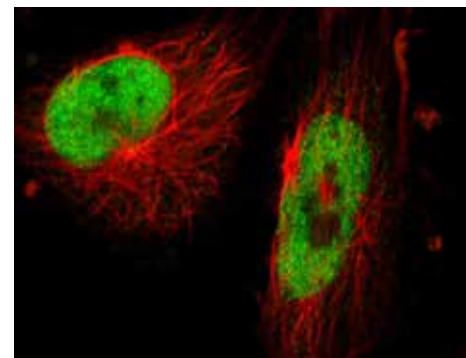
7. Smits A *et al.* GABA-A Channel Subunit Expression in Human Glioma Correlates with Tumor Histology and Clinical Outcome. *PLoS One* 2012 27(5):e37041. Epub 2012 May 17.
8. Leja J *et al.* Novel markers for enterochromaffin cells and gastrointestinal neuroendocrine carcinomas. *Mod Pathol* 2009 Feb;22(2):261-72.
9. Choi CH *et al.* Identification of differentially expressed genes according to chemosensitivity in advanced ovarian serous adenocarcinomas: expression of GRIA2 predicts better survival. *Br J Cancer* 2012 Jun 26;107(1):91-9.
10. Azizan EA *et al.* Somatic mutations in ATP1A1 and CACNA1D underlie a common subtype of adrenal hypertension. *Nat Genet* 2013 Sep;45(9):1055-60.
11. Kuga T *et al.* Lamin B2 prevents chromosome instability by ensuring proper mitotic chromosome segregation. *Oncogenesis* 2014 Mar 17;3:e94.



The gamma-aminobutyric acid (GABA) A receptor, alpha 3 (Anti-GABRA3) antibody (HPA000839) strongly labels fibers in various brain regions including the rat central amygdala.



The Anti-KIF11 antibody (HPA010568) against Kinesin family member 11 strongly labels fibers in human hippocampus tissue.



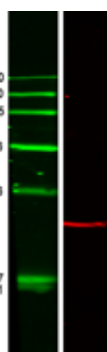
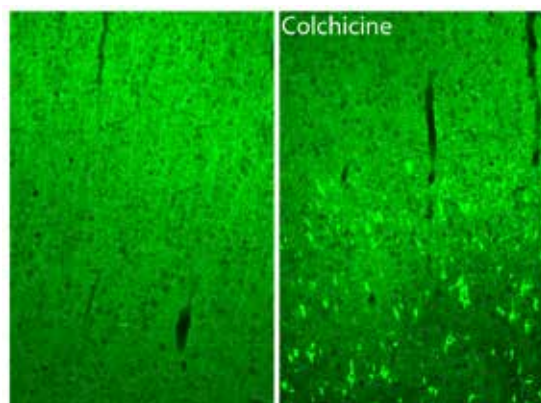
SIGNALING continued

| Product Name | Product Number | Applications (human tissues) | Antigen seq identity to mouse / rat |
|------------------------|-------------------------|------------------------------|-------------------------------------|
| Anti-KIF17 | HPA032085 | IHC, ICC-IF | 85 / 82% |
| Anti-KIF18A | HPA039312 | IHC, WB, ICC-IF | 80 / 82% |
| Anti-KIF1A | HPA005442 | IHC | 95 / 96% |
| Anti-KIF1C | HPA024602 | IHC, WB*, ICC-IF | 81 / 83% |
| Anti-KIF21B | HPA027249 | IHC | 91 / 93% |
| Anti-KIF26B | HPA028562 | IHC, ICC-IF | 88 / 80% |
| Anti-KIF4A (KIF4A & B) | HPA034745 | IHC, WB, ICC-IF | 64 / 63% |
| Anti-KIF5A | HPA004469 | IHC, WB* | 91 / 88% |
| Anti-KIF5C | HPA035210 | IHC, WB, ICC-IF | 100/100% |
| Anti-KIF7 | HPA043145 | IHC, WB | 69 / 69% |
| Anti-KIFAP3 | HPA023742 | IHC | 100 / 100% |
| Anti-KCNC2 | HPA019664 | IHC, WB | 71 / 99% |
| Anti-MAPK1 (ERK) | HPA030069 | IHC, WB, ICC-IF | 100 / 100% |
| Anti-MAPK3 (ERK1) | HPA005700 | IHC, WB* | 98 / 98% |
| Anti-MGLUR1 | HPA015701 | IHC | 80 / 80% |
| Anti-MGLUR7 | HPA036659 | IHC | 100 / 58% |
| Anti-MGLUR8 | HPA051481 | IHC | 95 / 90% |
| Anti-NCS1 | HPA019713 | IHC, WB, ICC-IF | 100 / 100% |
| Anti-PRKCA | HPA006563 | IHC, WB*, ICC-IF | 99 / 99% |
| Anti-PRKCH | HPA053709 | IHC, ICC-IF | 97 / 64% |
| Anti-PNMT | HPA051005 | IHC, WB | 89 / 92% |
| Anti-PRKACB (PKACB) | HPA029754 | IHC | 73 / 76% |
| Anti-PRKCZ | HPA021851 | IHC, WB | 94 / 94% |
| Anti-RAB3A | HPA003160 | IHC | 99 / 99% |
| Anti-RAP1GAP | HPA001922 | IHC, WB* | 92 / 91% |
| Anti-RAP1GAP2 | HPA022896 ¹² | IHC, WB*, ICC-IF | 94 / 95% |
| Anti-SLC17A6 (VGLUT2) | AMAb91981 | IHC | 85 / 85% |
| Anti-SLC17A6 (VGLUT2) | HPA039226 | IHC, WB | 85 / 85% |
| Anti-SLC17A7 (VGLUT1) | AMAb91041 | IHC, WB | 94 / 94% |
| Anti-SLC17A7 (VGLUT1) | HPA063679 | IHC, WB | 94 / 94% |
| Anti-SLC22A2 | AMAb90792 | IHC | 84 / 77% |
| Anti-SLC22A2 | HPA008567 ¹³ | IHC, WB | 84 / 77% |
| Anti-SLC32A1 (VGAT) | AMAb91943 | IHC | 95 / 93% |
| Anti-SLC32A1 (VGAT) | HPA058859 | IHC | 95 / 93% |

* WB both in human and rodent samples

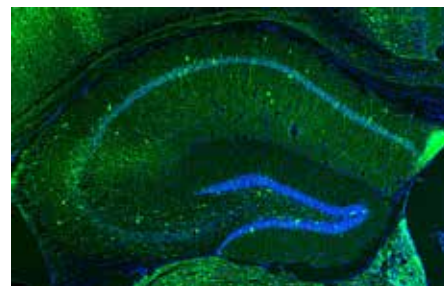
12. Jakobsen L *et al.* Novel asymmetrically localizing components of human centrosomes identified by complementary proteomics methods. *EMBO J* 2011 Apr 20; 30(8):1520-35. Epub 2011 Mar 11.

13. Shao R *et al.* Direct effects of metformin in the endometrium: a hypothetical mechanism for the treatment of women with PCOS and endometrial carcinoma. *J Exp Clin Cancer Res* 33(1):41. Epub 2014/05/11.

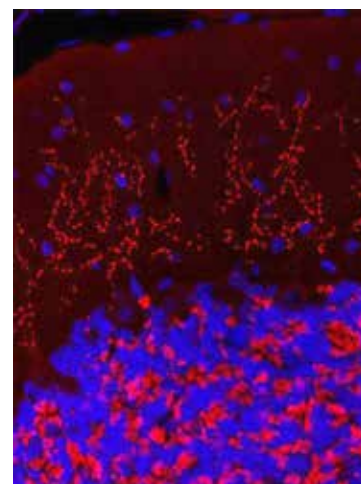


The Anti-SNAP25 antibody (HPA001830) against synaptosomal-associated protein 25 strongly labels the synaptic field in the rat somatosensory cortex. Inhibition of axonal transport with colchicine arrests SNAP25 in perikarya.

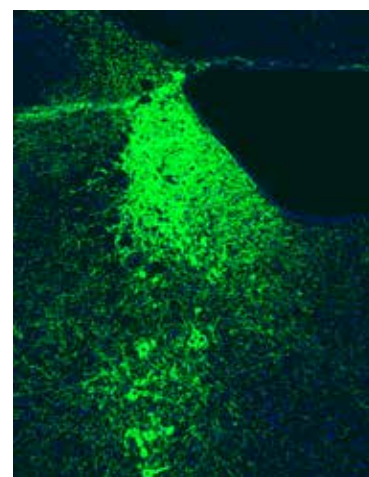
In Western Blot, the HPA001830 antibody recognizes a band of expected target size (23 kDa).



The GTPase-activating protein RAP1GAP is expressed in a subset of neurons including hippocampal interneurons in the mouse brain. This is illustrated using the Anti-RAP1GAP antibody (HPA001922).



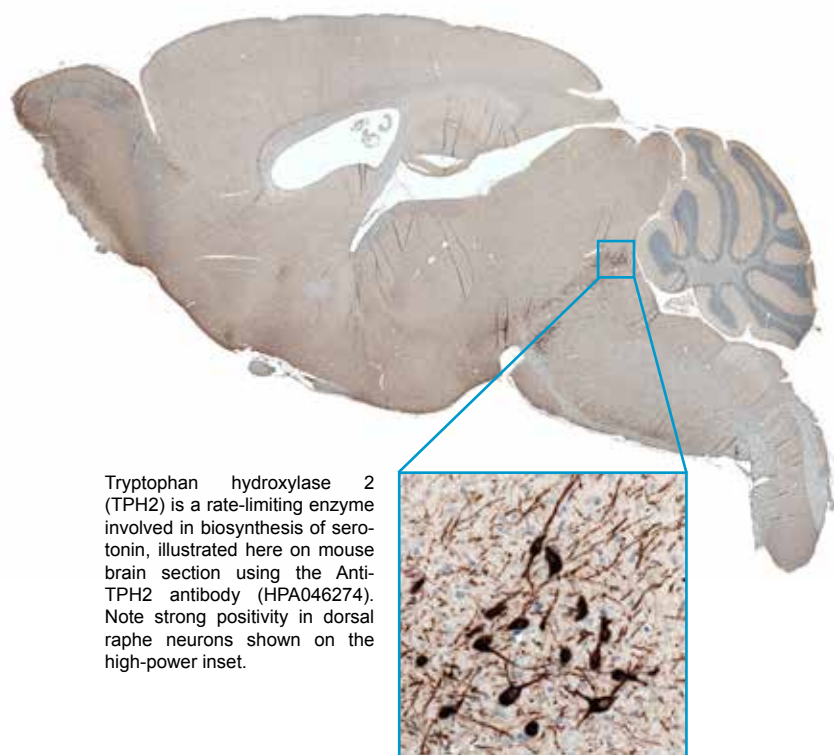
Vesicular glutamate transporter 2 (SLC17A6/VGLUT2) mediates the uptake of glutamate into synaptic vesicles at presynaptic nerve terminals. Here shown using the Anti-SLC17A6 antibody (HPA039226) on rat cerebellum section.



The noradrenaline transporter (NET/SLC6A2) is responsible for reuptake of noradrenaline into presynaptic nerve terminals and stains noradrenergic fibers throughout the brain and labels noradrenergic neurons in the rat locus coeruleus. Illustrated here by the Anti-SLC6A2/NET antibody (AMAb91116).

| Product Name | Product Number | Applications (human tissues) | Antigen seq identity to mouse / rat |
|-------------------|----------------------------|------------------------------|-------------------------------------|
| Anti-SLC6A2 (NET) | AMAb91116 | IHC | |
| Anti-SLC6A3 (DAT) | AMAb91125 | IHC | 85 / 85% |
| Anti-SLC6A3 (DAT) | HPA013602 | IHC,WB | 85 / 85% |
| Anti-SNAP25 | HPA001830 ¹⁴⁻¹⁶ | IHC,WB,ICC-IF | 100 / 100% |
| Anti-SNAP29 | HPA031823 | IHC | 89 / 92% |
| Anti-SST (SOM) | HPA019472 | IHC,WB | 98 / 98% |
| Anti-STXBP1 | HPA008209 | IHC,WB*,ICC-IF | 100 / 100% |
| Anti-STXBP5 | HPA039991 ¹⁷ | IHC,WB,ICC-IF | 98 / 98% |
| Anti-STXBP6 | HPA003552 | IHC,WB | 99 / 99% |
| Anti-SYNGR1 | HPA029673 | IHC | 90 / 88% |
| Anti-SYNPR | HPA061671 | IHC,WB | 97 / 97% |
| Anti-SYP | HPA002858 | IHC,WB | 83 / 83% |
| Anti-SYT1 | HPA008394 | IHC,WB | 100 / 100% |
| Anti-SYT12 | HPA011006 | IHC,WB* | 96 / 98% |
| Anti-SYT13 | HPA046224 | IHC | 96 / 93% |
| Anti-SYT14 | HPA036963 | IHC,WB*,ICC-IF | 87 / 27% |
| Anti-SYT16 | HPA004199 | IHC,WB | 95 / 95% |
| Anti-TGFA | HPA042297 | IHC,WB | 93 / 93% |
| Anti-TH | AMAb91112 | IHC | 88 / 88% |
| Anti-TH | HPA061003 | IHC | 88 / 88% |
| Anti-TPH2 (NTPH) | AMAb91108 | IHC | 100 / 100% |
| Anti-TPH2 (NTPH) | HPA046274 | IHC | 100 / 100% |
| Anti-VAMP4 | HPA050418 | IHC,WB,ICC-IF | 100 / 100% |
| Anti-VAMP7 | HPA036733 ¹⁸ | IHC,ICC-IF | 98 / 93% |

* WB both in human and rodent samples



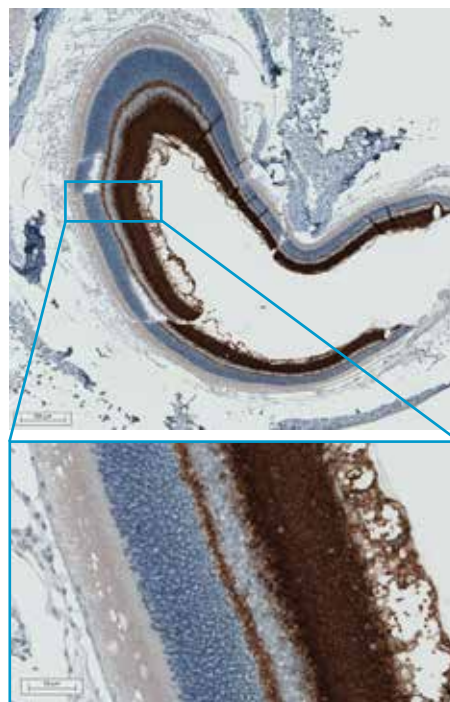
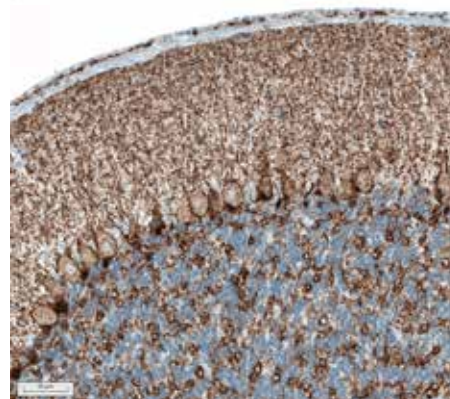
14. Mulder J *et al.* Tissue profiling of the mammalian central nervous system using human antibody-based proteomics. *Mol Cell Proteomics* 2009 Jul;8(7):1612-22.

15. Lindskog C *et al.* Novel pancreatic beta cell-specific proteins: antibody-based proteomics for identification of new biomarker candidates. *J Proteomics* 2012 May 17;75(9):2611-20.

16. Cardoso TC *et al.* Immunohistochemical approach to the pathogenesis of clinical cases of bovine Herpesvirus type 5 infections. *Diagn Pathol* 2010 Sep 10;5:57.

17. Ye S *et al.* Platelet secretion and hemostasis require syntaxin-binding protein STXBP5. *J Clin Invest* 2014/10/01 00:00; 124(10):4517-4528. Epub 2014/09/17.

18. Tannour-Louet M *et al.* Increased gene copy number of the vesicle SNARE VAMP7 disrupts human male urogenital development through altered estrogen action. *Nat Med* 2014/07/01 00:00; 20(7):715-724. Epub 2014/06/01.



Vesicular inhibitory amino acid transporter SLC32A1 is crucial for uptake of the inhibitory neurotransmitters GABA and glycine into the synaptic vesicles. The micrographs show strong immunoreactivity in rat cerebellar cortex and retina using the Anti-SLC32A1 antibody (HPA058859).

SIGNALING continued



Sodium-dependent dopamine transporter (SLC6A3, DAT) terminates action of dopamine by its re-uptake into pre-synaptic terminals. Immunohistochemical micrographs show dopaminergic system in mouse (upper) and rat (lower) brain using the Anti-DAT antibody (HPA013602). Note strong labelling of dopaminergic cell bodies in the substantia nigra and in terminals in the basal forebrain (insets).

NEURAL LINEAGE MARKERS

| Product Name | Product Number | Subcategory | Applications (human tissues) | Antigen seq identity to mouse / rat |
|--------------------|----------------------------|-------------------------|------------------------------|-------------------------------------|
| Anti-ACTN1 | HPA006035 | cytoskeleton | IHC,WB* | 98 / 99% |
| Anti-ACTN4 | HPA001873 | cytoskeleton | IHC,WB*,ICC-IF | 99 / 98% |
| Anti-AIF | HPA049234 ¹ | microglia | IHC | 84 / 84% |
| Anti-CALB1 (CB) | HPA023099 | calcium binding protein | IHC,WB,ICC-IF | 98 / 99% |
| Anti-CALB2 (CR) | HPA007305 | calcium binding protein | IHC,WB*,ICC-IF | 100 / 100% |
| Anti-CD68 | AMAb90874 | microglia | IHC,WB | 76 / 76% |
| Anti-CD68 | HPA048982 ² | microglia | IHC | 76 / 76% |
| Anti-CNP | AMAb91067 | oligodendrocytes | IHC,WB* | 76 / 77% |
| Anti-CNP | HPA023280 | oligodendrocytes | IHC,WB,ICC-IF | 76 / 77% |
| Anti-EZR | AMAb90976 | astroglia | IHC,WB,ICC-IF | 93 / 93% |
| Anti-EZR | HPA021616 ^{3,4} | astroglia | IHC,WB*,ICC-IF | 93 / 93% |
| Anti-GFAP | AMAb91033 | astrocytes | IHC,WB | 98 / 100% |
| Anti-GFAP | HPA056030 | astrocytes | IHC,WB | 98 / 100% |
| Anti-GLUL | AMAb91101 | astrocytes | IHC,WB* | 95 / 53% |
| Anti-GLUL | HPA007316 ^{5,6} | astrocytes | IHC,WB | 95 / 53% |
| Anti-ICAM5 | HPA009083 | adhesion molecule | IHC,ICC-IF | 85 / 86% |
| Anti-INA | HPA008057 | cytoskeleton | IHC,WB*,ICC-IF | 83 / 84% |
| Anti-ITGAM (CD11b) | AMAb90911 | microglia | IHC,WB | 67 / 68% |
| Anti-ITGAM | HPA002274 ^{7,8} | microglia | IHC,WB | 67 / 68% |
| Anti-MAP1A | HPA039064 | cytoskeleton | IHC | 60 / 52% |
| Anti-MAP1B | HPA022275 ⁹ | cytoskeleton | IHC,ICC-IF | 85 / 86% |
| Anti-MAP2 | HPA008273 ¹⁰ | cytoskeleton | IHC,ICC-IF | 96 / 96% |
| Anti-MBP | AMAb91062 | Schwann cells | IHC,WB | 97 / 97% |
| Anti-MBP | HPA049222 | Schwann cells | IHC,WB | 97 / 97% |
| Anti-MCAM | HPA008848 | adhesion molecule | IHC | 75 / 73% |
| Anti-MKI67 (Ki67) | AMAb90870 | progenitors | IHC | 68 / 68% |
| Anti-MKI67 (Ki67) | HPA000451 ^{11,12} | progenitors | IHC,ICC-IF | 66 / 67% |
| Anti-MOG | AMAb92066 | oligodendrocytes | IHC,WB | 91 / 89% |
| Anti-MOG | HPA021873 | oligodendrocytes | IHC,WB | 91 / 89% |
| Anti-MYO5A | HPA001356 | cytoskeleton | IHC,ICC-IF | 99 / 98% |

* WB both in human and rodent samples

1. Silva K *et al.* Cortical neurons are a prominent source of the proinflammatory cytokine osteopontin in HIV-associated neurocognitive disorders. *J Neurovirol* 2015/01/01 21(2):174-185. Epub 2015/01/31.

2. Antoine Louveau *et al.* Structural and functional features of central nervous system lymphatic vessels *Nature* June 01, 2015.

3. Andersson G *et al.* Reduced expression of ezrin in urothelial bladder cancer signifies more advanced tumours and an impaired survival: a validation study of two independent patient cohorts. *BMC Urol* 1/01/01 14:36. Epub 2014/05/12.

4. Antoine Louveau *et al.* Structural and functional features of central nervous system lymphatic vessels *Nature* June 01, 2015.

5. Perisic L *et al.* Profiling of atherosclerotic lesions by gene and tissue microarrays reveals PCSK6 as a novel protease in unstable carotid atherosclerosis. *Arterioscler Thromb Vasc Biol* , 2013 Oct; 33(10):2432-43. Epub 2013 Aug 1.

6. Ko YH *et al.* Glutamine fuels a vicious cycle of autophagy in the tumor stroma and oxidative mitochondrial metabolism in epithelial cancer cells: Implications for preventing chemotherapy resistance *Cancer Biol Ther* 2011/12/15 00:00; 12(12):1085-1097. Epub 2011/12/15.

7. Zibert JR *et al.* Halting angiogenesis by non-viral somatic gene therapy alleviates psoriasis and murine psoriasiform skin lesions. *J Clin Invest* 2011 Jan 4;121(1):410-21.

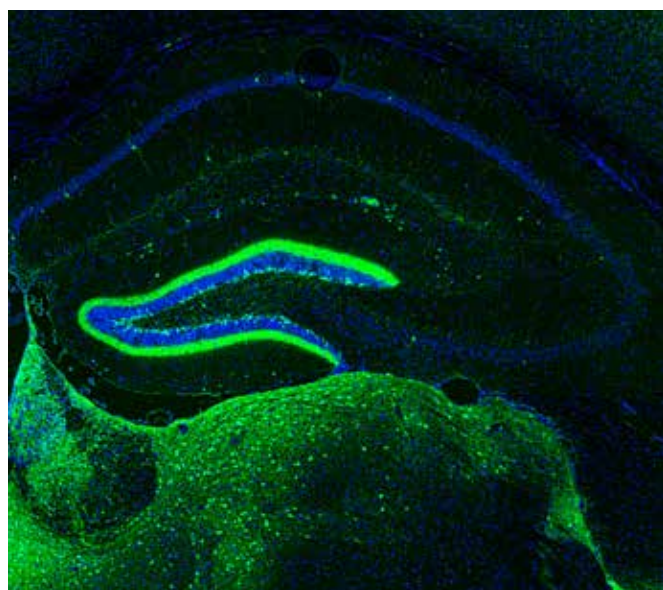
8. Pedersen ED *et al.* In situ deposition of complement in human acute brain ischaemia. *Scand J Immunol* 2009 Jun;69(6):555-62.

9. Claudio Isella *et al.* Stromal contribution to the colorectal cancer transcriptome. *Nature Genetics* February 23, 2015.

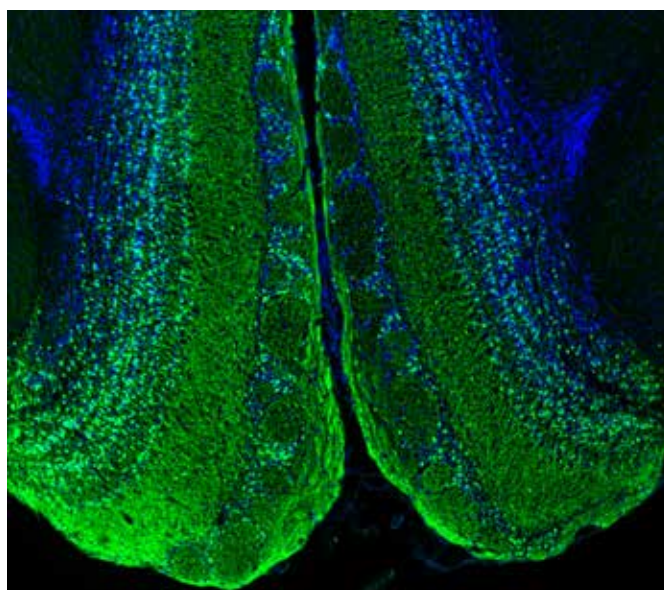
10. Lee DA *et al.* Tanycytes of the hypothalamic median eminence form a diet-responsive neurogenic niche. *Nat Neurosci* 2012 Mar 25;15(5):700-2.

11. Pohler E *et al.* Haploinsufficiency for AAGAB causes clinically heterogeneous forms of punctate palmoplantar keratoderma. *Nat Genet* 2012 Oct 14;44(11):1272-6.

12. Li S *et al.* Endothelial VEGF Sculptures Cortical Cytoarchitecture. *J Neurosci* 2013 Sep 11; 33(37):14809-14815.



Calretinin is a neuron specific EF-hand calcium binding protein expressed in subsets of neurons throughout the nervous system. The image shows the labeling of a mouse hippocampus and dorsal thalamus using the Anti-CALB2 antibody HPA007305. Note the strong labeling in the dentate gyrus.



Secretagogin is a newly discovered EF-hand calcium binding protein strongly expressed in the mouse olfactory bulb. Here visualized using the Anti-SCGN antibody HPA006641.

NEURAL LINEAGE MARKERS continued

| Product Name | Product Number | Subcategory | Applications (human tissues) | Antigen seq identity to mouse / rat |
|-------------------|-------------------------------|--------------------------------------|------------------------------|-------------------------------------|
| Anti-NCAM2 | HPA030900 ¹³ | adhesion molecule | IHC,ICC-IF | 89 / 91% |
| Anti-NECAB1 | AMAb90801 | calcium binding protein;interneurons | IHC,WB | 98 / 98% |
| Anti-NECAB1 | HPA023629 ¹⁴ | calcium binding protein;interneurons | IHC,WB | 98 / 98% |
| Anti-NECAB2 | AMAb90808 | calcium binding protein;interneurons | IHC | 85 / 84% |
| Anti-NECAB2 | HPA013998 ¹⁴ | calcium binding protein;interneurons | IHC,ICC-IF | 98 / 97% |
| Anti-NEFH (NF200) | AMAb91025 | neurons | IHC,WB | 88 / 94% |
| Anti-NEFH (NF200) | HPA061615 | neurons | IHC,ICC-IF | 88 / 94% |
| Anti-NEFM (NF160) | AMAb91027 | neurons | IHC,WB* | 98 / 98% |
| Anti-NEFM (NF160) | HPA022845 ^{15,16} | cytoskeleton | IHC | 98 / 98% |
| Anti-NLGN1 | HPA006680 | adhesion molecule | IHC,WB | 98 / 98% |
| Anti-PBK | HPA005753 | progenitors | IHC,WB*,ICC-IF | 91 / 94% |
| Anti-PTPRC | AMAb90518 | microgila | IHC,WB | 35 / 37% |
| Anti-PTPRC | HPA000440 ¹⁷ | microgila | IHC,WB | 35 / 37% |
| Anti-RBFOX3 | HPA030790 ^{18,19} | neuron nuclear marker | IHC,WB,ICC-IF | 93 / 94% |
| Anti-S100A8 | HPA024372 | macrophages | HC,WB | 56 / 60% |
| Anti-S100B | AMAb91038 | astrocytes | IHC,WB | 99 / 98% |
| Anti-S100B | HPA015768 ²⁰⁻²² | S100 calcium binding protein B | IHC,WB,ICC-IF | 99 / 98% |
| Anti-SCGN | AMAb90630 ²³ | calcium binding protein;interneurons | IHC,WB | 96 / 96% |
| Anti-SCGN | HPA006641 ^{14,24,25} | calcium binding protein;interneurons | IHC | 96 / 96% |
| Anti-UCHL1 | AMAb91145 | neurons | IHC,WB* | 97 / 97% |
| Anti-UCHL1 | HPA005993 ²⁷ | neurons | IHC,WB*,ICC-IF | 97 / 97% |

* WB both in human and rodent samples

13. Rodrigues RM *et al.* Human Skin-Derived Stem Cells as a Novel Cell Source for In Vitro Hepatotoxicity Screening of Pharmaceuticals. *Stem Cells Dev* 2014/01/01 23(1):44-55. Epub 2013/08/17.

14. Zhang MD *et al.* Neuronal calcium-binding proteins 1/2 localize to dorsal root ganglia and excitatory spinal neurons and are regulated by nerve injury. *Proc Natl Acad Sci U S A* 2014 Mar 25;111(12):E1149-58.

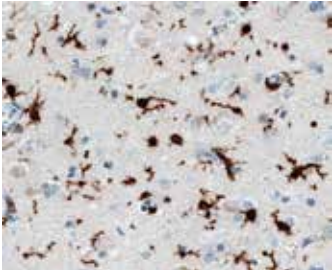
15. Häggmark A *et al* Plasma profiling reveals three proteins associated to amyotrophic lateral sclerosis. *Ann Clin Transl Neurol*, 2014/08/01; 1(8):544-553. Epub 2014/07/14.

16. Bachmann J *et al.* Affinity Proteomics Reveals Elevated Muscle Proteins in Plasma of Children with Cerebral Malaria. *PLoS Pathog* 1/01/01 10(4):e1004038. Epub 2014/04/17.

17. Edlund K *et al.* CD99 is a novel prognostic stromal marker in non-small cell lung cancer. *Int J Cancer* 2012 Nov 15; 131(10):2264-73. Epub 2012 Apr 24.

18. Bergmann O *et al.* The age of olfactory bulb neurons in humans. *Neuron* 2012 May 24;74(4):634-9.

19. Huttner HB *et al.* The age and genomic integrity of neurons after cortical stroke in humans. *Nat Neurosci* 2014 Jun; 17(6):801-3. Epub 2014 Apr 20.



The Anti-Allograft inflammatory factor 1 (AIF1) antibody (HPA049234) shows immunoreactivity in the microglia cells in human cortex.

20. Chaichana KL *et al.* Intra-operatively obtained human tissue: protocols and techniques for the study of neural stem cells. *J Neurosci Methods*. 2009 May 30;180(1):116-25.

21. Kielar M *et al.* Mutations in Eml1 lead to ectopic progenitors and neuronal heterotopia in mouse and human. *Nat Neurosci* 2014 Jul; 17(7):923-33. Epub 2014 May 25.

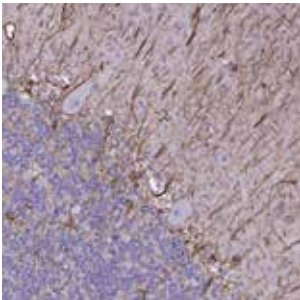
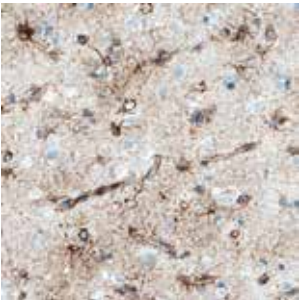
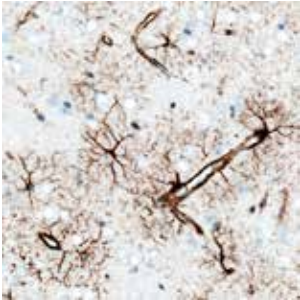
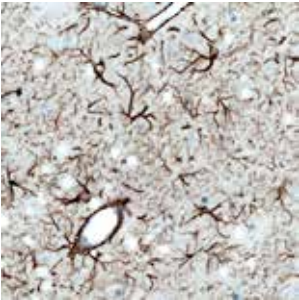
22. Darcy MJ *et al* Age-Dependent Role for Ras-GRF1 in the Late Stages of Adult Neurogenesis in the Dentate Gyrus. *Hippocampus* 2014/03/01 24(3):315-325.

23. Shi TJ *et al.* Secretagogin is expressed in sensory CGRP neurons and in spinal cord of mouse and complements other calcium-binding proteins, with a note on rat and human. *Mol Pain* 2012 Oct 29;8:80.

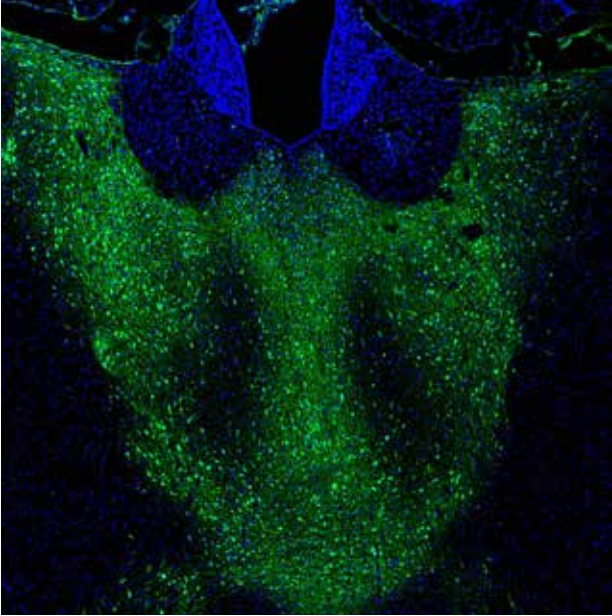
24. Mulder J *et al.* Secretagogin is a Ca2+-binding protein specifying subpopulations of telencephalic neurons. *Proc Natl Acad Sci U S A* 2009/12/29; 106(52):22492-22497. Epub 2009/12/16.

25. Attems J *et al.* Clusters of secretagogin-expressing neurons in the aged human olfactory tract lack terminal differentiation. *Proc Natl Acad Sci U S A* , 2012 Apr 17; 109(16):6259-64. Epub 2012 Apr 2.

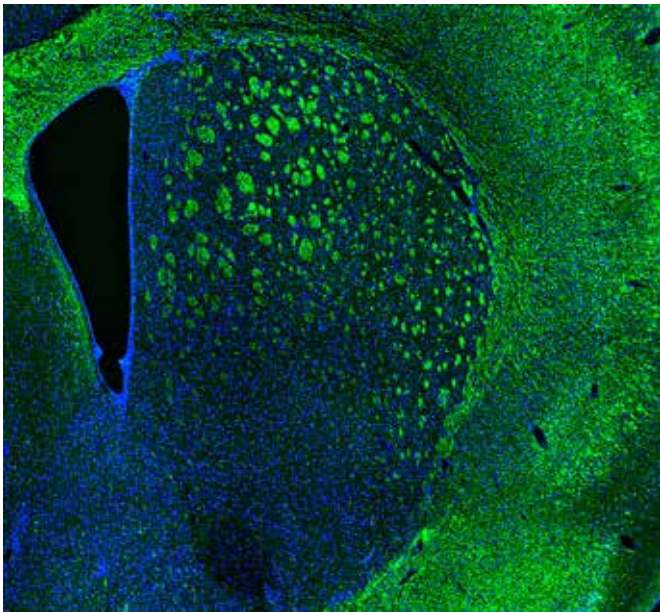
27. Lindskog C *et al.* Antibody-based proteomics for discovery and exploration of proteins expressed in pancreatic islets. *Discov Med* 2010 Jun; 9(49):565-78.



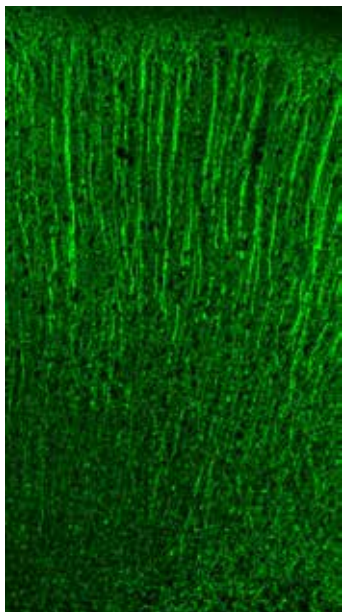
Glial fibrillary acidic protein (GFAP) is a cell-specific marker for astrocytes. Here illustrated by the Anti-GFAP antibody HPA056030 in rat cerebral cortex (upper left), mouse cerebral cortex (upper right), human cerebral cortex (lower left) and human cerebellum (lower right) tissue.



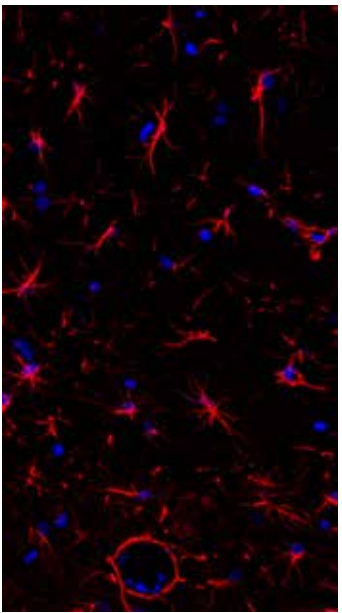
Distribution of NECAB1 (green) in the mouse dorsal medial thalamus. The PreciSA Monoclonal Anti-NECAB1 antibody AMAb90801 strongly labels neurons and their processes in the paraventricular and mediodorsal thalamic nuclei. Blue is the nuclear staining Hoechst.



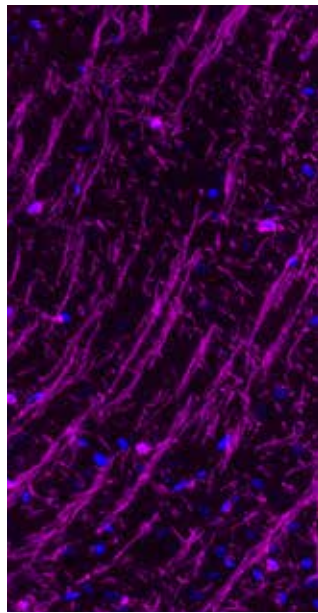
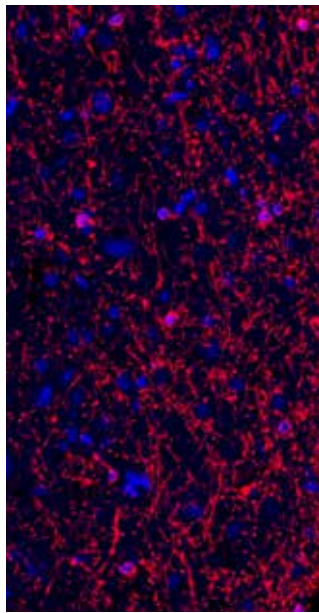
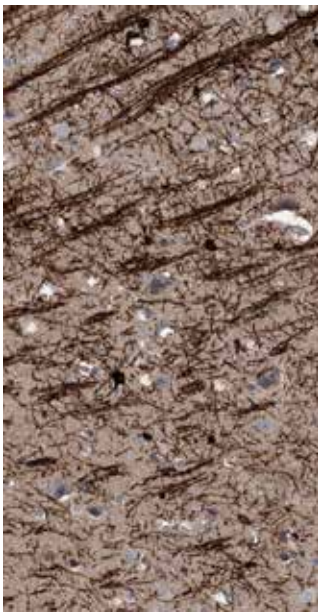
The image shows Anti-INA antibody (HPA008057) targeting internexin neuronal intermediate filament protein alpha (INA). Note the strong labeling of axons in striatal nerve bundles in the mouse brain.



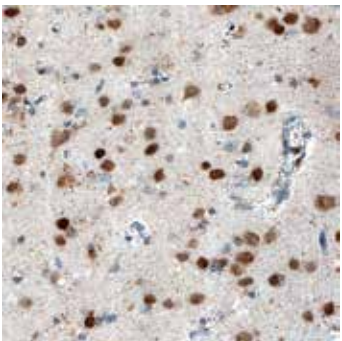
Anti-MAP2 antibody (HPA008273) against microtubule-associated protein 2 (MAP2) strongly labels dendrites in the mouse cortex.



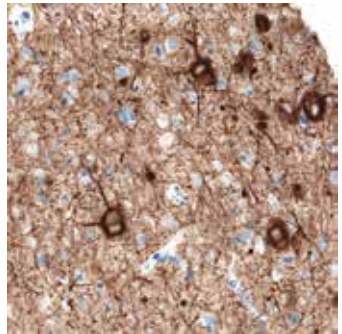
Glial fibrillary acidic protein (GFAP) is a cell specific marker distinguishing astrocytes from the other glial cells in the central nervous system. Labelling with the Anti-GFAP antibody HPA056030 shows astrocytes in rat cerebral cortex.



2',3'-cyclic-nucleotide 3'-phosphodiesterase (CNP) is a marker for oligodendrocytes in the central nervous system. Illustrated here by the Anti-CNP antibody HPA023280 (IHC) and HPA023266 (IF) in human cerebral cortex (left, middle) and in rat cerebral cortex (right).



RBFOX3 (=NeuN) is a neuronal specific nuclear protein which can be used to distinguish neurons from glial cells in tissue cultures and sections. Illustrated here by staining with the Anti-RBFOX3 antibody (HPA030790) in human cerebral cortex.



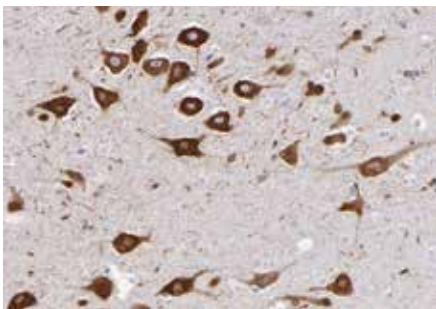
The Anti-Neurofilament medium polypeptide (NEFM) antibody (HPA022845) shows positivity in a subset of neuronal cells in human cerebral cortex.



AGING AND NEUROLOGICAL DISORDERS

| Product Name | Product Number | Applications (human tissues) | Antigen seq identity to mouse / rat |
|---------------------|----------------------------|------------------------------|-------------------------------------|
| Anti-ADAR | AMAb90535 | IHC, WB | 86 / 85% |
| Anti-ADAR | HPA003890 ¹⁻³ | IHC, WB, ICC-IF | 86 / 85% |
| Anti-AIMP1 | HPA018476 | IHC, WB*, ICC-IF | 96 / 97% |
| Anti-AOX1 | HPA040199 | IHC, ICC-IF | 84 / 86% |
| Anti-APBA1 | HPA019850 | IHC, WB* | 95 / 95% |
| Anti-APBA3 | HPA045577 | IHC, WB, ICC-IF | 70 / 68% |
| Anti-APBB2 | HPA023542 | IHC, WB, ICC-IF | 85 / 83% |
| Anti-APBB3 | HPA005571 | IHC, WB, ICC-IF | 84 / 84% |
| Anti-APP | HPA001462 ⁴ | IHC, ICC-IF | 95 / 95% |
| Anti-AQP4 | AMAb90537 | IHC, WB | 93 / 92% |
| Anti-AQP4 | HPA014784 | IHC, WB* | 93 / 92% |
| Anti-ATF2 | HPA022134 | IHC, WB*, ICC-IF | 99 / 99% |
| Anti-ATF3 | AMAb90909 | IHC | 92 / 92% |
| Anti-ATF3 | HPA001562 | IHC, WB*, ICC-IF | 92 / 92% |
| Anti-ATXN1 | HPA008335 | IHC, ICC-IF | 81 / 81% |
| Anti-ATXN2 | HPA018295 | IHC, WB*, ICC-IF | 90 / 91% |
| Anti-C3 | HPA020432 | IHC | 78 / 23% |
| Anti-CASP3 | HPA002643 ⁵ | IHC, WB*, ICC-IF | 84 / 88% |
| Anti-COX1 | HPA002834 ⁶ | IHC, WB | 93 / 90% |
| Anti-COX2/PTGS2 | HPA001335 ⁷⁻⁹ | IHC | 88 / 88% |
| Anti-CTSB | HPA018156 ^{10,11} | IHC, WB*, ICC-IF | 79 / 79% |
| Anti-CTSD | HPA003001 ¹² | IHC, WB | 86 / 86% |
| Anti-CXorf27 | HPA003356 | IHC | 47 / 46% |
| Anti-FBXO7 (PARK15) | HPA032114 | IHC | 78 / 81% |
| Anti-GSK3B | HPA028017 | IHC, WB*, ICC-IF | 100 / 100% |
| Anti-HIP1 | HPA017964 | IHC, WB | 79 / 77% |
| Anti-HTRA2 (PARK13) | HPA027366 | IHC, WB | 57 / 63% |
| Anti-ITGAM (CD11b) | AMAb90911 | IHC, WB | 67 / 68% |
| Anti-ITGAM (CD11b) | HPA002274 ^{13,14} | IHC, WB | 67 / 68% |
| Anti-ITM2B | HPA029292 | IHC, WB, ICC-IF | 95 / 96% |
| Anti-LRP1 | HPA022903 | IHC, WB, ICC-IF | 93 / 92% |
| Anti-LRP2 | HPA005980 ¹⁵ | IHC | 78 / 36% |
| Anti-MSR1 | HPA000272 | IHC, WB | 60 / 59% |
| Anti-NFKB1 | HPA027305 | IHC, WB, ICC-IF | 60 / 62% |
| Anti-OPTN | HPA003360 ¹⁶ | IHC, WB, ICC-IF | 64 / 68% |
| Anti-PADI4 | HPA017007 | IHC, WB | 66 / 69% |
| Anti-PARK7 | HPA004190 ¹⁷ | IHC, WB* | 89 / 90% |

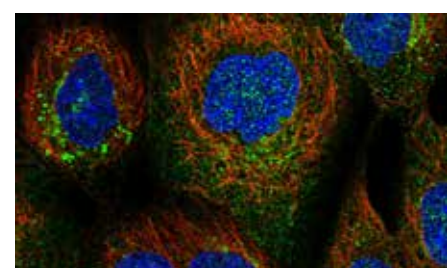
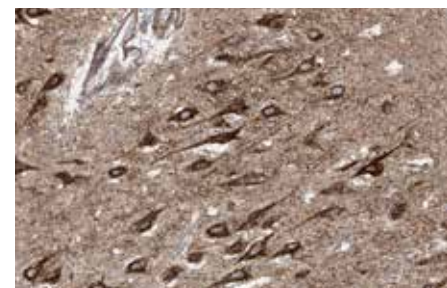
* WB both in human and rodent samples



Prostaglandin-endoperoxide synthase 1 (PTGS1) is strongly expressed in perikarya from hippocampal neurons (human tissue). Here shown using the Anti-COX1 (HPA002834) antibody.



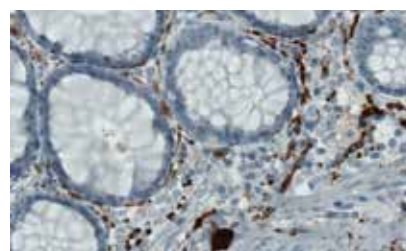
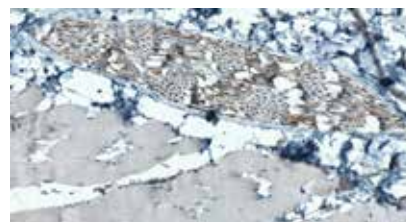
The Anti-ITM2B antibody (HPA029292), targeting Integral membrane protein 2B, strongly labels the soma and processes of hippocampal neurons (human tissue). Note the labeling of the Golgi apparatus in A-431 cells.



- Rice GI *et al.* Mutations in ADAR1 cause Aicardi-Goutières syndrome associated with a type I interferon signature. *Nat Genet* 2012 Nov;44(11):1243-8.
- Nachmani D *et al.* MicroRNA Editing Facilitates Immune Elimination of HCMV Infected Cells. *PLoS Pathog* 2014 210(2):e1003963. Epub 2014/02/27.
- Witman NM *et al.* ADAR-related activation of adenosine-to-inosine RNA editing during regeneration. *Stem Cells Dev* 2013 Aug 15;22(16):2254-67.
- Wu CC *et al.* Candidate serological biomarkers for cancer identified from the secretomes of 23 cancer cell lines and the human protein atlas. *Mol Cell Proteomics* 2010 Jun;9(6):1100-17.
- Contin MA *et al.* Photoreceptor damage induced by low-intensity light: model of retinal degeneration in mammals. *Mol Vis* , 1/01/01; 19:1614-1625. Epub 2013/07/25.
- Asplund A *et al.* Expression profiling of microdissected cell populations selected from basal cells in normal epidermis and basal cell carcinoma. *Br J Dermatol* 2008 Mar;158(3):527-38.
- Núñez F *et al.* Wnt/beta-catenin signaling enhances cyclooxygenase-2 (COX2) transcriptional activity in gastric cancer cells. *PLoS One* 2011 Apr 6;6(4):e18562.
- Charo C *et al.* PGE2 Regulates Pancreatic Stellate Cell Activity Via The EP4 Receptor. *Pancreas* 2013 Apr; 42(3):467-474.
- Charo C *et al.* Prostaglandin E2 regulates pancreatic stellate cell activity via the EP4 receptor. *Pancreas* 2013 Apr; 42(3):467-74.
- Wang H *et al.* Heterogeneity in signaling pathways of gastroenteropancreatic neuroendocrine tumors: a critical look at notch signaling pathway. *Mod Pathol* 2013 Jan;26(1):139-47.
- Perisic L *et al.* Profiling of atherosclerotic lesions by gene and tissue microarrays reveals PCSK6 as a novel protease in unstable carotid atherosclerosis. *J Transl Med*. 2011 Jul 21;9:114.
- Ahmad Y *et al.* (2011) Systematic analysis of protein pools, isoforms and modifications affecting turnover and subcellular localisation. *Mol Cell Proteomics* Mar;11(3):M111.013680.
- Zibert JR *et al.* Halting angiogenesis by non-viral somatic gene therapy alleviates psoriasis and murine psoriasisform skin lesions. *J Clin Invest* 2011 Jan 4;121(1):410-21.
- Pedersen ED *et al.* In situ deposition of complement in human acute brain ischaemia. *J Transl Med* 2009 Jul 21;9:114.
- Ma LJ *et al.* Angiotensin type 1 receptor modulates macrophage polarization and renal injury in obesity. *Am J Physiol Renal Physiol* 2011 May; 300(5):F1203-F1213. Epub 2011 Mar 2.
- Smith AM *et al.* Disruption of macrophage pro-inflammatory cytokine release in Crohn's disease is associated with reduced optineurin expression in a subset of patients *Immunology* 2015/01/01; 144(1):45-55. Epub 2014/12/08.
- Toyoda Y *et al.* Products of the Parkinson's disease-related glyoxalase DJ-1, D-lactate and glycolate, support mitochondrial membrane potential and neuronal survival. *Biol Open* 3(8):777-784. Epub 2014/07/25.

| Product Name | Product Number | Applications (human tissues) | Antigen seq identity to mouse / rat |
|---------------|-------------------------------|------------------------------|-------------------------------------|
| Anti-PHGDH | AMAb90786 | IHC, WB | 99 / 99% |
| Anti-PHGDH | HPA021241 ¹⁸⁻²¹ | IHC, WB*, ICC-IF | 99 / 99% |
| Anti-PRNP | HPA042754 | IHC | 91 / 91% |
| Anti-PSEN1 | HPA030760 | IHC | 82 / 81% |
| Anti-RHOT1 | AMAb90852 | IHC, WB | 100 / 100% |
| Anti-RHOT1 | HPA010687 ²²⁻²⁴ | IHC, WB | 100 / 100% |
| Anti-S100A8 | HPA024372 | IHC, WB | 56 / 60% |
| Anti-SERPINA3 | HPA002560 ^{25,26} | IHC, WB | 60 / 59% |
| Anti-SNCB | HPA035876 | IHC, WB, ICC-IF | 97 / 97% |
| Anti-SOD1 | HPA001401 ^{27,28} | IHC, WB*, ICC-IF | 82 / 81% |
| Anti-SOD2 | HPA001814 ^{29,30,31} | IHC, WB | 88 / 87% |
| Anti-THY1 | AMAb90844 | IHC, WB | 64 / 68% |
| Anti-THY1 | HPA003733 | IHC | 64 / 68% |
| Anti-TNFRSF21 | HPA006746 | IHC, WB | 86 / 85% |
| Anti-UBE2K | HPA028869 | IHC, ICC-IF | 100 / 100% |
| Anti-UCHL1 | HPA005993 ³² | IHC, WB*, ICC-IF | 97 / 97% |
| Anti-WHSC1 | AMAb90851 | IHC, WB | 91 / 91% |
| Anti-WHSC1 | HPA015801 ³³ | IHC, WB*, ICC-IF | 91 / 91% |
| Anti-VWF | AMAb90928 | IHC, WB | 80 / 80% |
| Anti-VWF | HPA002082 ^{34,35} | IHC | 82 / 78% |

* WB both in human and rodent samples



Ubiquitin-carboxyl-terminal hydrolase isozyme L1 (UCHL1, PGP9.5) is expressed in the neuronal cells of the central and peripheral nervous system. Expression of this protein is down-regulated in Parkinson's and in Alzheimer's disease patients. The micrographs show expression of UCHL1 protein in the peripheral nervous system (skin nerve and local nerves in colon) of human using the Anti-UCHL1 antibody HPA005993.

18. Possemato R *et al.* (2011) Functional genomics reveal that the serine synthesis pathway is essential in breast cancer. *Nature*. Aug 18;476(7360):346-50.

19. Maddocks OD *et al.* (2013) Serine starvation induces stress and p53-dependent metabolic remodelling in cancer cells. *Nature*. Jan 24;493(7433):542-6.

20. Nilsson LM *et al.* (2012) Mouse genetics suggests cell-context dependency for Myc-regulated metabolic enzymes during tumorigenesis. *PLoS Genet* 8(3):e1002573.

21. Mattaini KR *et al.* An epitope tag alters phosphoglycerate dehydrogenase structure and impairs ability to support cell proliferation. *Cancer Metab* 1/01/01; 3:5. Epub 2015/04/29.

22. Bingol B *et al.* The mitochondrial deubiquitinase USP30 opposes parkin-mediated mitophagy. *Nature* 2014 Jun 19; 510(7505):370-5. Epub 2014 Jun 4.

23. Birsa N *et al.* Lysine 27 Ubiquitination of the Mitochondrial Transport Protein Miro Is Dependent on Serine 65 of the Parkin Ubiquitin Ligase. *J Biol Chem* 2014/05/23; 289(21):14569-14582. Epub 2014/03/26.

24. De Vos KJ *et al.* VAPB interacts with the mitochondrial protein PTP1P51 to regulate calcium homeostasis. *Hum Mol Genet* 2012 Mar 15; 21(6):1299-311. Epub 2011 Nov 30.

25. Häggmark A *et al.* (2013) Antibody-based profiling of cerebrospinal fluid within multiple sclerosis. *Proteomics* Aug;13(15):2256-67.

26. Bannon MJ *et al.* A Molecular Profile of Cocaine Abuse Includes the Differential Expression of Genes that Regulate Transcription, Chromatin, and Dopamine Cell Phenotype *Neuropsychopharmacology* 2014/08/01; 39(9):2191-2199. Epub 2014/04/16.

27. Filézac de L'Etang A *et al.* Marinesco-Sjögren syndrome protein SIL1 regulates motor neuron subtype-selective ER stress in ALS *Nature Neuroscience* January 05, 2015.

28. Miettinen TP *et al.* NQO2 Is a Reactive Oxygen Species Generating Off-Target for Acetaminophen. *Mol Pharm* 2014/12/01; 11(12):4395-4404. Epub 2014/10/14.

29. Arimappamagan A *et al.* (2013) A Fourteen Gene GBM Prognostic Signature Identifies Association of Immune Response Pathway and Mesenchymal Subtype with High Risk Group. *PLoS ONE* 2013-04-30.

30. Lindfors C *et al.* (2011) Hypothalamic mitochondrial dysfunction associated with anorexia in the anx/anx mouse. *Proc Natl Acad Sci U S A*. Nov 1;108(44):18108-13.

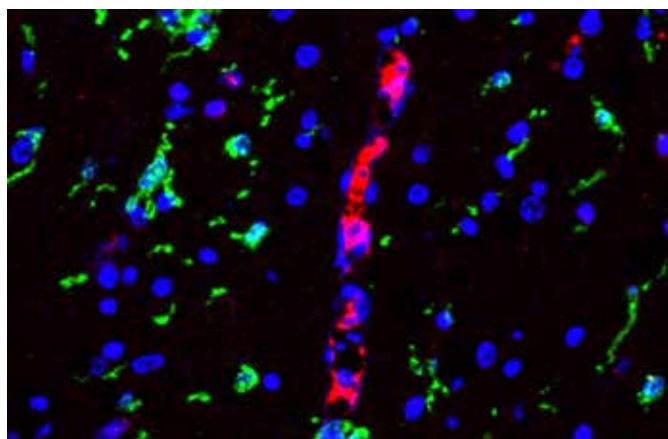
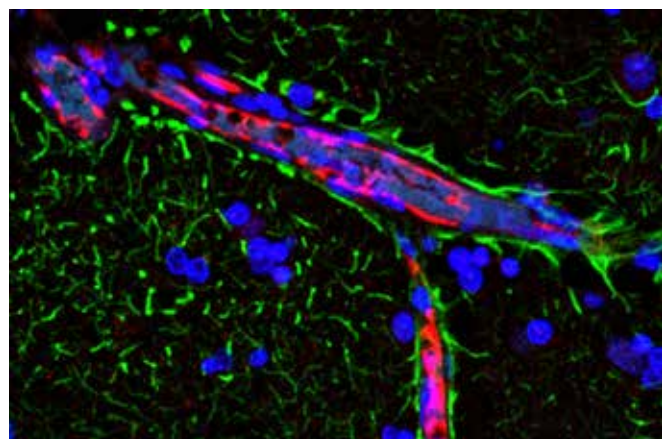
31. Mulder J *et al.* (2009) Tissue profiling of the mammalian central nervous system using human antibody-based proteomics. *Mol Cell Proteomics*. Jul;8(7):1612-22.

32. Lindskog C *et al.* (2010) Antibody-based proteomics for discovery and exploration of proteins expressed in pancreatic islets. *Discov Med* Jun;9(49):565-78.

33. Toyokawa G *et al.* Histone Lysine Methyltransferase Wolf-Hirschhorn Syndrome Candidate 1 Is Involved in Human Carcinogenesis through Regulation of the Wnt Pathway. *Neoplasia* 2011/10/01; 13(10):887-898.

34. Bachmann J *et al.* (2014) Affinity proteomics reveals elevated muscle proteins in plasma of children with cerebral malaria. *PLoS Pathog*. Apr;10(4):e1004038.

35. Chakraborty G *et al.* (2012) Semaphorin 3A suppresses tumor growth and metastasis in mice melanoma model. *PLoS One* 7(3):e33633.



Complement component C3 plays an important role in the activation of complement system and has been associated with neuro-inflammation. The Anti-C3 antibody (HPA020432) strongly labels capillaries in MS affected brain tissue. (Blue = Hoechst, Green = IBA1 or GFAP (clone GA5), Red = C3).

DEVELOPMENT

| Product Name | Product Number | Applications (human tissues) | Antigen seq identity to mouse / rat |
|-------------------|----------------------------|------------------------------|-------------------------------------|
| Anti-BMP3 | HPA045344 | IHC,WB | 74 / 75% |
| Anti-ENG | AMAb90925 | IHC | 66 / 22% |
| Anti-ENG | HPA011862 ¹ | IHC,WB,ICC-IF | 66 / 22% |
| Anti-FABP7 | AMAb90595 | IHC,WB | 89 / 90% |
| Anti-FABP7 | HPA028825 ^{2,3} | IHC,WB | 89 / 90% |
| Anti-FLT1 | AMAb90704 | IHC,WB | 80 / 82% |
| Anti-FLT1 | HPA014290 | IHC | 77 / 78% |
| Anti-GAP43 | HPA015600 ⁴ | IHC,WB | 71 / 70% |
| Anti-GLI3 | HPA005534 | IHC,ICC-IF,WB | 74 / 76% |
| Anti-MEF2C | AMAb90727 | IHC,WB | 97 / 47% |
| Anti-MEF2C | HPA005533 ⁵⁻⁸ | IHC,WB,ICC-IF | 97 / 47% |
| Anti-MKI67 (Ki67) | HPA000451 ^{9,10} | IHC,ICC-IF | 66 / 67% |
| Anti-NACC1 | HPA021238 | IHC,ICC-IF | 91 / 89% |
| Anti-NES (Nestin) | AMAb90556 | IHC,WB | 47 / 42% |
| Anti-NES (Nestin) | HPA007007 ¹¹ | IHC,WB,ICC-IF | 47 / 42% |
| Anti-NKX2-2 | HPA003468 ^{12,13} | IHC,WB | 96 / 97% |
| Anti-PAX6 | HPA030775 | IHC,ICC-IF | 100 / 100% |
| Anti-PBK | HPA005753 | IHC,WB*,ICC-IF | 91 / 94% |

* WB both in human and rodent samples

1. Ziebarth AJ *et al.* Endoglin (CD105) contributes to platinum resistance and is a target for tumor-specific therapy in epithelial ovarian cancer. *Clin Cancer Res* 2013 Jan 1; 19(1):170-182. Epub 2012/11/12.

2. Tan C *et al.* Impact of Gender in Renal Cell Carcinoma: The Relationship of FABP7 and BRN2 Expression with Overall Survival. *Clin Med Insights Oncol* 2014 2821-27. Epub 2014/02/23.

3. Gromov P *et al* FABP7 and HMGCS2 Are Novel Protein Markers for Apocrine Differentiation Categorizing Apocrine Carcinoma of the Breast. *PLoS One* 1/01/01; 9(11):e112024. Epub 2014/11/12.

4. Häggmark A *et al.* Antibody-based profiling of cerebrospinal fluid within multiple sclerosis. *Proteomics* 2013 Aug;13(15):2256-67.

5. Yelamanchili SV *et al.* MicroRNA-21 dysregulates the expression of MEF2C in neurons in monkey and human SIV/HIV neurological disease. *Cell Death Dis* 2010;1:e77.

6. Wirrig EE *et al.* Differential expression of cartilage and bone-related proteins in pediatric and adult diseased aortic valves. *J Mol Cell Cardiol* 2011 Mar; 50(3):561-569. Epub 2010 Dec 14.

7. Clark CD *et al.* Evolutionary Conservation of Nkx2.5 Autoregulation in the Second Heart Field. *Dev Biol* 2013 Feb 1; 374(1):198-209. Epub 2012/11/17.

8. Lockhart MM *et al* Mef2c Regulates Transcription of the Extracellular Matrix Protein Cartilage Link Protein 1 in the Developing Murine Heart. *PLoS One* 8(2):e57073. Epub 2013/02/26.

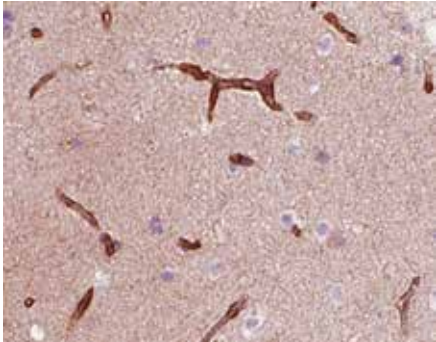
9. Li S *et al.* Endothelial VEGF Sculpts Cortical Cytoarchitecture. *J Neurosci* 2013 Sep 11; 33(37):14809-14815.

10. Pohler E *et al.* Haploinsufficiency for AAGAB causes clinically heterogeneous forms of punctate palmoplantar keratoderma. *Nat Genet* 2012 Oct 14;44(11):1272-6.

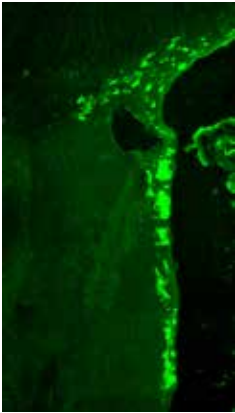
11. Sellheyer K *et al.* Spatiotemporal expression pattern of neuroepithelial stem cell marker nestin suggests a role in dermal homeostasis, neovasculogenesis, and tumor stroma development: a study on embryonic and adult human skin. *J Am Acad Dermatol* 2010 Jul;63(1):93-113.

12. Lawson MH *et al.* Two novel determinants of etoposide resistance in small cell lung cancer. *Cancer Res* 2011 Jul 15;71(14):4877-87.

13. Pasquali L *et al.* Pancreatic islet enhancer clusters enriched in type 2 diabetes risk-associated variants. *Nat Genet* 2014 Feb;46(2):136-43.



Immunohistochemical staining using the Anti-NES (Nestin) antibody AMAb90556 of human cerebral cortex shows strong immunoreactivity in the endothelial cells.



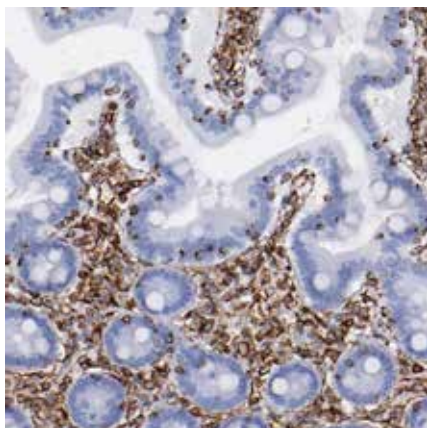
PDZ binding kinase (PBK) is expressed in neural progenitors in both the dentate gyrus and subventricular zone of the lateral ventricle in the adult rat. Here visualized using the Anti-PBK antibody (HPA005753).



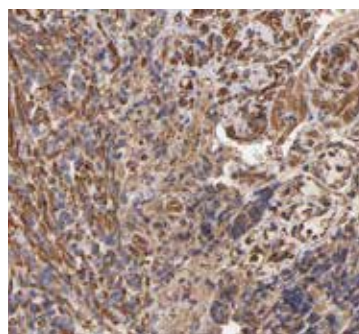
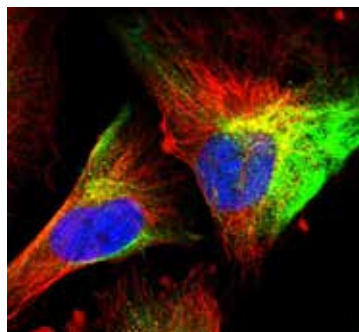
DNA-binding protein SATB2 is required for initiation of the upper-layer neurons specific genetic program and for inactivation of deep-layer neurons specific genes. Here illustrated by Anti-SATB2 antibody AMAb90679 in rat brain. Note strong nuclear immunoreactivity in cerebral cortex and in the CA1 layer of the hippocampus and absence of positivity in the dentate gyrus.

| Product Name | Product Number | Applications (human tissues) | Antigen seq identity to mouse / rat |
|---------------------|----------------------------|------------------------------|-------------------------------------|
| Anti-REST | AMAb90740 | IHC | 41 / 43% |
| Anti-RUNX1 | HPA004176 ¹⁴ | IHC,WB,ICC-IF | 93 / 93% |
| Anti-RUNX2 | AMAb90591 | IHC,WB | 100 / 81% |
| Anti-RUNX2 | HPA022040 ^{15,16} | IHC,WB,ICC-IF | 100 / 81% |
| Anti-SATB2 | AMAb90679 | IHC,WB | 100 / 100% |
| Anti-SATB2 | HPA029543 ¹⁷ | IHC,ICC-IF | 100 / 100% |
| Anti-SOX4 | HPA029901 | IHC,ICC-IF | 100 / 39% |
| Anti-SOX6 | HPA001923 ^{18,19} | IHC,WB,ICC-IF | 96 / 96% |
| Anti-SOX7 | HPA009065 ^{20,21} | IHC,WB | 91 / 91% |
| Anti-SOX11 | AMAb90502 ²² | IHC,WB | 82 / 82% |
| Anti-SOX11 | HPA000536 ²³⁻²⁷ | IHC,WB | 82 / 82% |
| Anti-SOX30 | HPA006159 | IHC,WB | 68 / 70% |
| Anti-THY1 | AMAb90844 | IHC,WB | 64 / 68% |
| Anti-THY1 | HPA003733 | IHC | 64 / 68% |
| Anti-TM4SF2/TSPAN7 | HPA003140 ^{28,29} | IHC,WB | 96 / 96% |
| Anti-TM4SF2/TSPAN7 | AMAb90621 | IHC,WB | 96 / 96% |
| Anti-VIM (vimentin) | AMAb90516 | IHC,WB | 99 / 99% |
| Anti-VIM | HPA001762 ³⁰ | IHC,WB*,ICC-IF | 99 / 99% |

* WB both in human and rodent samples



Immunohistochemical staining using the Anti-VIM (Vimentin) antibody HPA001762 of human duodenum shows distinct positivity in mesenchymal and lymphoid cells (upper left). In glioma tissue, immunoreactivity is strong in tumor cells (lower right). Immunofluorescent staining of human cell line U-251MG shows positivity in cytoskeleton (upper right).



14. Ferrari N *et al.* Expression of RUNX1 Correlates with Poor Patient Prognosis in Triple Negative Breast Cancer. *PLoS One* 1/01/01; 9(6):e100759. Epub 2014/06/26.

15. Martínez-Abadías N *et al.* From shape to cells: mouse models reveal mechanisms altering palate development in Apert syndrome. *Dis Model Mech* 2013 May; 6(3):768-779. Epub 2013/03/08.

16. McDonald L *et al.* RUNX2 correlates with subtype-specific breast cancer in a human tissue microarray, and ectopic expression of Runx2 perturbs differentiation in the mouse mammary gland. *Dis Model Mech* 2014/05/01; 7(5):525-534. Epub 2014/03/13.

17. Nodin B *et al.* Molecular correlates and prognostic significance of SATB1 expression in colorectal cancer. *Diagn Pathol* 2012 Aug 30;7:115.

18. Herlofson SR *et al.* Chondrogenic Differentiation of Human Bone Marrow-Derived Mesenchymal Stem Cells in Self-Gelling Alginate Discs Reveals Novel Chondrogenic Signature Gene Clusters. *Tissue Eng Part A*. 2010 Apr; 17(7-8):1003-1013. Epub 2010 Dec 27.

19. Fernandes AM *et al.* Similar Properties of Chondrocytes from Osteoarthritis Joints and Mesenchymal Stem Cells from Healthy Donors for Tissue Engineering of Articular Cartilage. *PLoS One* 1/01/01; 8(5):e62994. Epub 2013/05/09.

20. Saegusa M *et al.* Sox4 functions as a positive regulator of beta-catenin signaling through upregulation of TCF4 during molecular differentiation of endometrial carcinomas. *Lab Invest* 2012 Apr;92(4):511-21.

21. Hayano T *et al.* SOX7 is down-regulated in lung cancer. *J Exp Clin Cancer Res* 2013 232(1):17. Epub 2013/04/04.

22. Soldini D *et al.* Assessment of SOX11 Expression in Routine Lymphoma Tissue Sections: Characterization of New Monoclonal Antibodies for Diagnosis of Mantle Cell Lymphoma. *Am J Surg Pathol* 2014 Jan;38(1):86-93.

23. Aiden AP *et al.* Wilms tumor chromatin profiles highlight stem cell properties and a renal developmental network. *Cell Stem Cell* 2010 Jun 4;6(6):591-602.

24. Wang X *et al.* Gene expression profiling and chromatin immunoprecipitation identify DBN1, SETMAR and HIG2 as direct targets of SOX11 in mantle cell lymphoma. *PLoS One* 2010 Nov 22;5(11):e14085.

25. Fernández V *et al.* Genomic and gene expression profiling defines indolent forms of mantle cell lymphoma. *Cancer Res* 2010 Feb 15;70(4):1408-18.

26. Sernbo S *et al.* The tumour suppressor SOX11 is associated with improved survival among high grade epithelial ovarian cancers and is regulated by reversible promoter methylation. *BMC Cancer* 2011 Sep 24;11:405.

27. Davidson B *et al.* The clinical role of epithelial-mesenchymal transition and stem cell markers in advanced-stage ovarian serous carcinoma effusions. *Hum Pathol* 2015 Jan; 46(1):1-8.

28. Wuttig D *et al.* CD31, EDNRB and TSPAN7 are promising prognostic markers in clear-cell renal cell carcinoma revealed by genome-wide expression analyses of primary tumors and metastases. *Int J Cancer* 2012 Sep 1; 131(5):E693-704. Epub 2012 Feb 28.

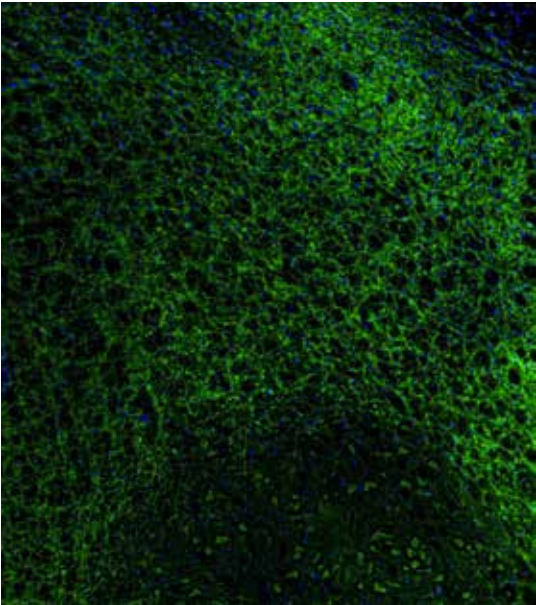
29. Lindskog C *et al.* Antibody-based proteomics for discovery and exploration of proteins expressed in pancreatic islets. *Discov Med* 2010 Jun; 9(49):565-78.

30. Yamasaki T *et al.* Tumor suppressive microRNA-138 contributes to cell migration and invasion through its targeting of vimentin in renal cell carcinoma. *Int J Oncol* 2012 241(3):805-817. Epub 2012/07/03.

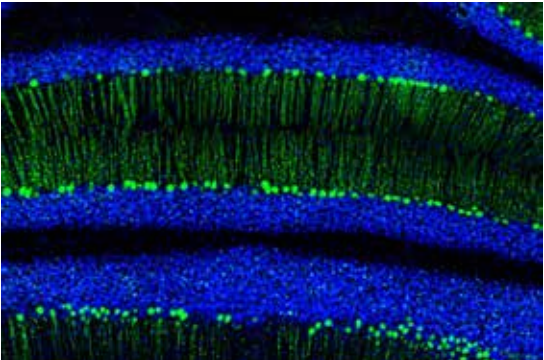


Antibodies on HPA Mouse Brain Atlas

| Product Name | Product Number | Validated Applications | Antigen seq identity to mouse / rat |
|---------------|--------------------------|------------------------|-------------------------------------|
| Anti-AMPD2 | HPA045760 | IHC,WB,ICC-IF | 99% / 99% |
| Anti-AQP4 | HPA014784 | IHC,WB | 93% / 92% |
| Anti-ARFGEF1 | HPA023822 | IHC,WB,ICC-IF | 90% / 90% |
| Anti-ARHGAP1 | HPA004689 ¹ | IHC,WB,ICC-IF | 98% / 98% |
| Anti-BCAR1 | HPA042282 | IHC,WB,ICC-IF | 75% / 93% |
| Anti-BCL11B | HPA049117 | IHC | 96% / 48% |
| Anti-BIRC3 | HPA002317 ²⁻⁴ | IHC,WB,ICC-IF | 75% / 74% |
| Anti-C17orf75 | HPA004061 ⁵ | IHC,WB,ICC-IF | 84% / 83% |
| Anti-C21orf59 | HPA028849 | IHC,WB | 95% / 93% |
| Anti-CALB2 | HPA007305 ³ | IHC,WB,ICC-IF | 98% / 98% |
| Anti-CAMK2B | HPA026307 | IHC,WB | 96% / 96% |
| Anti-DDX3X | HPA001648 ^{3,6} | IHC,WB | 97% / 97% |
| Anti-DPP6 | HPA050509 | IHC,WB | 86% / 86% |
| Anti-DTX4 | HPA059294 | IHC,ICC-IF | 86% / 33% |
| Anti-ECH1 | HPA005835 ³ | IHC,WB | 78% / 81% |
| Anti-EIF1AY | HPA002561 | IHC,WB | 99% / 99% |
| Anti-FAM213B | HPA006403 | IHC,WB | 92% / 89% |
| Anti-FGF3 | HPA012692 | IHC,ICC-IF | 80% / 81% |
| Anti-FH | HPA025770 | IHC,WB,ICC-IF | 99% / 100% |
| Anti-FOXO1 | HPA001252 ^{5,7} | IHC | 91% / 90% |
| Anti-FRMD6 | HPA001297 ⁸ | IHC,WB,ICC-IF | 94% / 94% |
| Anti-GABRA3 | HPA000839 ³ | IHC,WB | 91% / 93% |
| Anti-GFAP | HPA056030 | IHC,WB | 98% / 100% |
| Anti-GKAP1 | HPA035117 | IHC,WB,ICC-IF | 93% / 93% |
| Anti-GMFB | HPA002954 ⁹ | IHC,WB | 97% / 94% |
| Anti-GOLGA5 | HPA000992 ¹⁰ | IHC,WB,ICC-IF | 70% / 76% |



Immunofluorescence IHC staining of mouse medulla with Anti-GABRA3 antibody (HPA000839) shows strong immunoreactivity in neuronal processes and cell bodies.



Immunohistochemical staining of mouse cerebellum with Anti-CAMK2B antibody (HPA026307) shows neuronal positivity in Purkinje cells.

1. Härmä V *et al.* Lysophosphatidic acid and sphingosine-1-phosphate promote morphogenesis and block invasion of prostate cancer cells in three-dimensional organotypic models. *Oncogene* 22012 Apr 19;31(16):2075-89.

2. Jones DR *et al.* Phase I Trial of Induction Histone Deacetylase and Proteasome Inhibition Followed by Surgery in Non-small Cell Lung Cancer. *J Thorac Oncol* 2012 Nov; 7(11):1683-1690.

3. Mulder J *et al.* Tissue profiling of the mammalian central nervous system using human antibody-based proteomics. *Mol Cell Proteomics* 2009 8(7):1612-22.

4. Almubarak H *et al.* Zoledronic acid directly suppresses cell proliferation and induces apoptosis in highly tumorigenic prostate and breast cancers. *J Carcinog* 2011 Jan 15;10:2.

5. Kato BS *et al.* Variance decomposition of protein profiles from antibody arrays using a longitudinal twin model. *Proteome Sci* 9:73. Epub 2011/11/17.

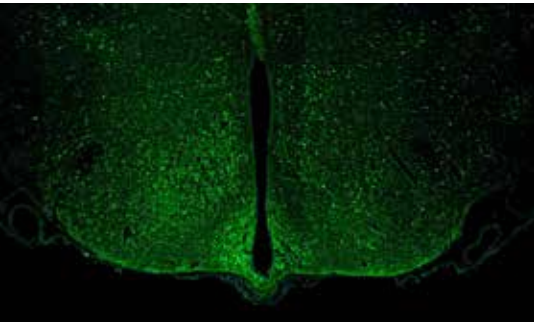
6. Hagerstrand D *et al.* Systematic interrogation of 3q26 identifies TLOC1 and SKIL as cancer drivers. *Cancer Discov* 2013/09/01 3(9):1044-1057. Epub 2013/06/13.

7. Sahu B *et al.* Dual role of FoxA1 in androgen receptor binding to chromatin, androgen signalling and prostate cancer. *EMBO J* 2011/10/05 30(19):3962-3976. Epub 2011/09/13.

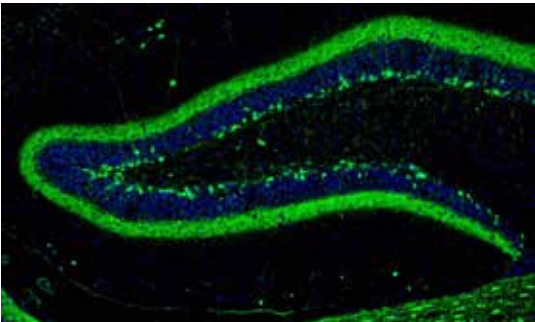
8. De Sousa E *et al.* Poor-prognosis colon cancer is defined by a molecularly distinct subtype and develops from serrated precursor lesions. *Nat Med* 2013 May;19(5):614-8.

9. Yu Y *et al.* Evaluation of blastomere biopsy using a mouse model indicates the potential high risk of neurodegenerative disorders in the offspring. *Mol Cell Proteomics* 2009 Jul;8(7):1490-500.

10. Hsu YC *et al.* Multiple domains in the Crumbs Homolog 2a (Crb2a) protein are required for regulating rod photoreceptor size. *BMC Cell Biol* 2010 Jul 29;11:60.



Immunohistochemical staining of mouse hypothalamus with Anti-CALB antibody (HPA007305) shows selective staining in a subset of neurons and fibers in the accruate nucleus.



Immunohistochemical staining of mouse hippocampus Anti-CALB antibody (HPA007305) shows selective staining in subsets of neurons and fibers in dentate gyrus.

| Product Name | Product Number | Validated Applications | Antigen seq identity to mouse / rat |
|--------------|----------------------------|------------------------|-------------------------------------|
| Anti-HSPA2 | HPA000798 ¹¹⁻¹³ | IHC,WB | 95% / 95% |
| Anti-IER5 | HPA029894 | IHC,WB,ICC-IF | 86% / 33% |
| Anti-INA | HPA008057 ³ | IHC,WB,ICC-IF | 83% / 84% |
| Anti-ITPKA | HPA040454 | IHC,WB,ICC-IF | 91% / 89% |
| Anti-KIF5A | HPA004469 | IHC,WB | 91% / 88% |
| Anti-LIAS | HPA018842 | IHC,WB,ICC-IF | 89% / 92% |
| Anti-LRPAP1 | HPA008001 ³ | IHC,WB,ICC-IF | 81% / 80% |
| Anti-MAP2 | HPA012828 ^{14,15} | IHC,ICC-IF | 91% / 89% |
| Anti-MARS | HPA004125 ¹⁶ | IHC,WB,ICC-IF | 92% / 92% |
| Anti-MBP | HPA049222 | IHC,WB | 97% / 97% |
| Anti-NAGLU | HPA038815 | IHC | 88% / 89% |
| Anti-NDUFV2 | HPA003404 ¹⁷ | IHC,WB | 95% / 95% |
| Anti-NECAB1 | HPA023629 ¹⁸ | IHC,WB | 98% / 98% |
| Anti-NECAB2 | HPA013998 ¹⁸ | IHC,ICC-IF | 98% / 97% |
| Anti-NPAS2 | HPA019674 | IHC,WB,ICC-IF | 85% / 87% |
| Anti-OGFOD1 | HPA003215 ^{19,20} | IHC,WB,ICC-IF | 80% / 81% |
| Anti-OTUB1 | HPA039176 | IHC,WB,ICC-IF | 100% / 100% |
| Anti-PBK | HPA005753 | IHC,WB,ICC-IF | 91% / 94% |
| Anti-PCP4 | HPA005792 ²¹⁻²⁴ | IHC,WB | 96% / 96% |
| Anti-PPP1R1B | HPA048630 | IHC,WB | 87% / 91% |
| Anti-QK1 | HPA019123 | IHC,WB,ICC-IF | 100% / 100% |
| Anti-RABGGTB | HPA026585 | IHC,WB,ICC-IF | 97% / 96% |
| Anti-RAP1GAP | HPA001922 | IHC,WB | 92% / 91% |
| Anti-RCN2 | HPA030694 | IHC,WB,ICC-IF | 91% / 90% |
| Anti-RPL9 | HPA003372 ^{3,25} | IHC,WB,ICC-IF | 99% / 98% |

11. Scieglinska D *et al.* Expression, function, and regulation of the testis-enriched heat shock HSPA2 gene in rodents and humans *Cell Stress Chaperones* 2015/03/01 20(2):221-235. Epub 2014/10/25.

12. Rogon C *et al.* HSP70-binding protein HSPBP1 regulates chaperone expression at a posttranslational level and is essential for spermatogenesis. *Mol Biol Cell* 2014/08/01 25(15):2260-2271.

13. Grad I *et al.* The Molecular Chaperone Hsp90α Is Required for Meiotic Progression of Spermatocytes beyond Pachytene in the Mouse. *PLoS One* 5(12):e15770. Epub 2010/12/31.

14. Andersson S *et al.* Antibodies Biotinylated Using a Synthetic Z-domain from Protein A Provide Stringent In Situ Protein Detection *J Histochem Cytochem* 2013/11/01 61(11):773-784.

15. Pontén F *et al.* The Human Protein Atlas-a tool for pathology. *J Pathol* 2008 Dec;216(4):387-93.

16. van Meel E *et al.* Rare recessive loss-of-function methionyl-tRNA synthetase mutations presenting as a multi-organ phenotype. *BMC Med Genet* 2013 214106. Epub 2013/10/08.

17. Choi J *et al.* A Novel PGC-1α Isoform in Brain Localizes to Mitochondria and Associates with PINK1 and VDAC. *Biochem Biophys Res Commun* 2013/06/14 435(4):671-677. Epub 2013/05/17.

18. Zhang MD *et al.* Neuronal calcium-binding proteins 1/2 localize to dorsal root ganglia and excitatory spinal neurons and are regulated by nerve injury. *Proc Natl Acad Sci U S A* 2014 Mar 25;111(12):E1149-58.

19. Loenarz C *et al.* Hydroxylation of the eukaryotic ribosomal decoding center affects translational accuracy. *Proc Natl Acad Sci U S A* 2014/03/18 111(11):4019-4024. Epub 2014/02/18.

20. Wehner KA *et al.* OGFOD1, a novel modulator of eukaryotic translation initiation factor 2α phosphorylation and the cellular response to stress. *Mol Cell Biol* 2010 Apr;30(8):2006-16.

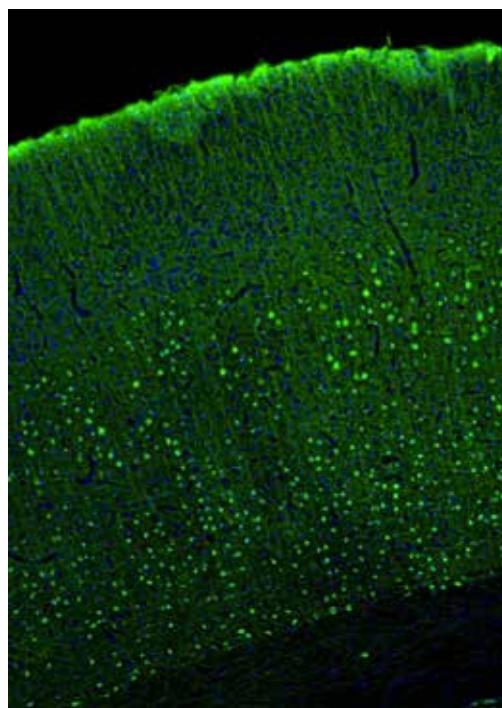
21. Valero M *et al.* Determinants of different deep and superficial CA1 pyramidal cell dynamics during sharp-wave ripples. *Nature Neuroscience* July 27, 2015.

22. Hitti FL *et al.* The hippocampal CA2 region is essential for social memory. *Nature* 2014/04/03 508(7494):88-92. Epub 2014/02/23.

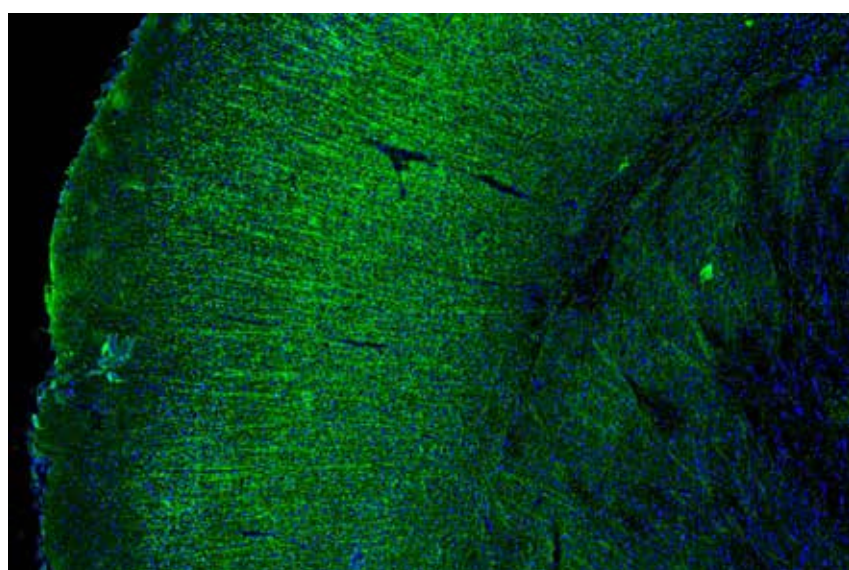
23. Kohara K *et al.* Cell type-specific genetic and optogenetic tools reveal hippocampal CA2 circuits. *Nat Neurosci* 2014 Feb; 17(2):269-79. Epub 2013 Dec 15.

24. Botcher NA *et al.* Distribution of interneurons in the CA2 region of the rat hippocampus. *Front Neuroanat* 8:104. Epub 2014/09/26.

25. Badhai J *et al.* Posttranscriptional down regulation of small ribosomal subunit proteins correlates with reduction of 18S rRNA in RPS19 deficiency. *FEBS Lett* 2009/06/18 583(12):2049-2053. Epub 2009/05/18.



Immunofluorescence IHC staining of mouse cerebral cortex with Anti-PCP4 antibody (HPA005792) shows strong immunoreactivity in neuronal cell bodies in the deep cortical layers.



Immunohistochemical staining of mouse cerebral cortex with Anti-MBP antibody (HPA049222) shows strong staining in myelinated fibres.

| Product Name | Product Number | Validated Applications | Antigen seq identity to mouse / rat |
|--------------|----------------------------|------------------------|-------------------------------------|
| Anti-SAYSD1 | HPA007959 | IHC,WB,ICC-IF | 92% / 32% |
| Anti-SCGN | HPA006641 ²⁶⁻²⁹ | IHC | 96% / 96% |
| Anti-SEMA3E | HPA029419 | IHC | 86% / 86% |
| Anti-SLC2A1 | HPA031345 | IHC | 100% / 100% |
| Anti-SSR3 | HPA014906 | IHC,WB | 100% / 43% |
| Anti-SST | HPA019472 | IHC,WB | 98% / 98% |
| Anti-SYNJ2BP | HPA000866 | IHC,WB,ICC-IF | 96% / 95% |
| Anti-TH | HPA061003 | IHC | 88% / 88% |
| Anti-TXNL1 | HPA002828 | IHC,WB,ICC-IF | 98% / 98% |
| Anti-UBTF | HPA006385 ³⁰ | IHC,WB,ICC-IF | 98% / 98% |
| Anti-USP11 | HPA037536 | IHC,ICC-IF | 82% / 83% |
| Anti-USP48 | HPA030046 | IHC,WB,ICC-IF | 95% / 94% |
| Anti-ZNF3 | HPA003719 | IHC,ICC-IF | 77% / 78% |

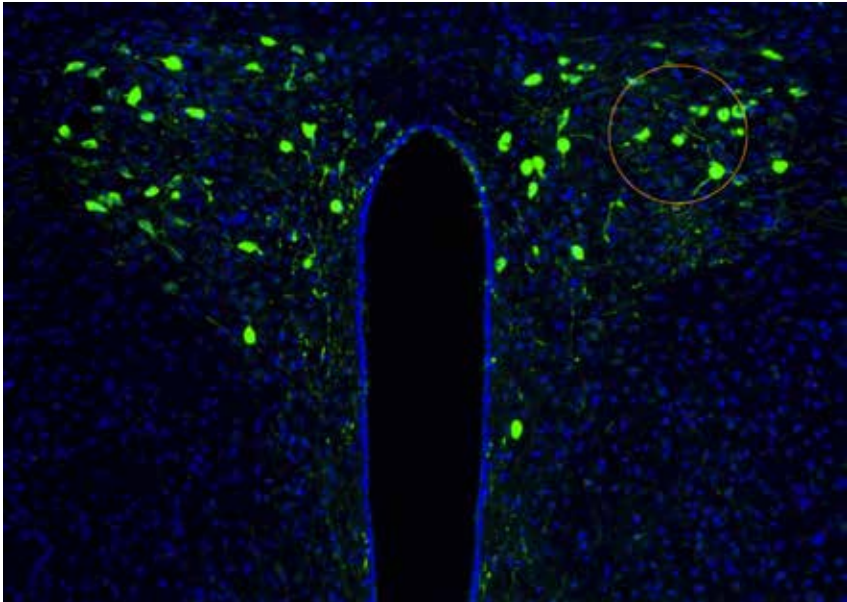
26. Zhang MD *et al.* Neuronal calcium-binding proteins 1/2 localize to dorsal root ganglia and excitatory spinal neurons and are regulated by nerve injury. *Proc Natl Acad Sci U S A* 2014 Mar 25;111(12):E1149-58.

27. Mulder J *et al.* Secretagogin is a Ca2+-binding protein identifying prospective extended amygdala neurons in the developing mammalian telencephalon. *Eur J Neurosci* 2010 Jun;31(12):2166-77.

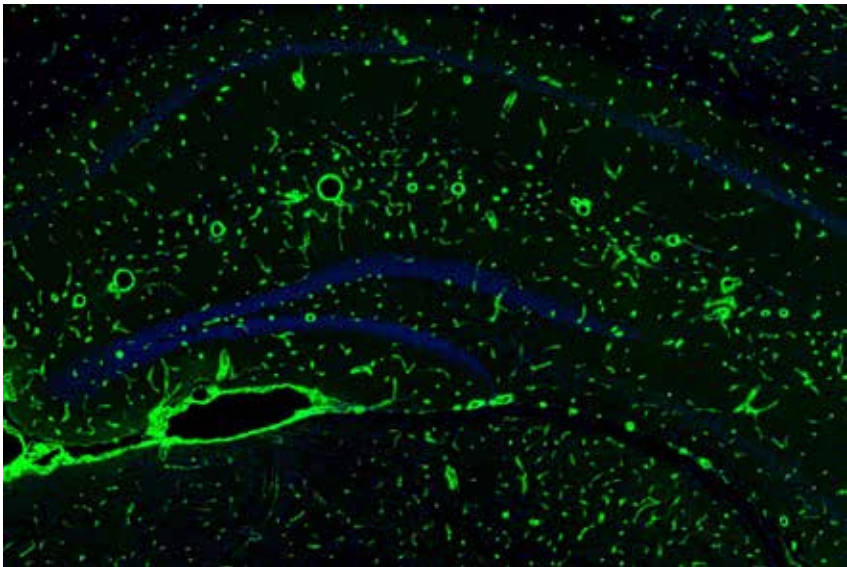
28. Attems J *et al.* Clusters of secretagogin-expressing neurons in the aged human olfactory tract lack terminal differentiation. *Proc Natl Acad Sci U S A* 2012 Apr 17;109(16):6259-64.

29. Alpár A *et al.* The renaissance of Ca2+-binding proteins in the nervous system: secretagogin takes center stage. *Cell Signal* 2012 Feb;24(2):378-87.

30. Sobol M *et al.* UBF complexes with phosphatidylinositol 4,5-bisphosphate in nucleolar organizer regions regardless of ongoing RNA polymerase I activity. *Nucleus* 2013 Nov 1; 4(6):478-486. Epub 2013/12/05.



Immunofluorescence IHC staining of mouse hypothalamus with Anti-SAYSD1 antibody (HPA007959) shows selective neuronal staining in the paraventricular nucleus.



Immunohistochemical staining of mouse hippocampus Anti-SLC2A1 antibody (HPA031345) shows strong staining in endothelial cells.



REFERENCES

- Mulder J, Björling E, Jonasson K, Wernérus H, Hober S, Hökfelt T, Uhlén M.
Tissue profiling of the mammalian central nervous system using human antibody-based proteomics.
Mol Cell Proteomics 2009 8(7):1612-22.
- Mulder J, Wernérus H, Shi TJ, Pontén F, Hober S, Uhlén M, Hökfelt T.
Systematically generated antibodies against human gene products: high throughput screening on sections from the rat nervous system.
Neuroscience 2007 Jun 8;146(4):1689-703.
- Uhlén M, Oksvold P, Fagerberg L, Lundberg E, Jonasson K, Forsberg M, Zwahlen M, Kampf C, Wester K, Hober S, Wernérus H, Björling L, Pontén F.
Towards a knowledge-based Human Protein Atlas.
Nat Biotechnol 2010 28(12):1248-50.
- Fagerberg L, Strömberg S, El-Obeid A, Gry M, Nilsson K, Uhlén M, Pontén F, Asplund A.
Large-scale protein profiling in human cell lines using antibody-based proteomics.
J Proteome Res. 2011 10(9):4066-75.
- Kopp UC, Cicha MZ, Smith LA, Mulder J, Hökfelt T.
Renal sympathetic nerve activity modulates afferent renal nerve activity by PGE2-dependent activation of alpha1- and alpha2-adrenoceptors on renal sensory nerve fibers.
Am J Physiol Regul Integr Comp Physiol. 2007 Oct;293(4):R1561-72. Epub 2007 Aug 15.
- Lindfors C, Nilsson IA, Garcia-Roves PM, Zuberi AR, Karimi M, Donahue LR, Roopenian DC, Mulder J, Uhlén M, Ekström TJ, Davisson MT, Hökfelt TG, Schalling M, Johansen JE.
Hypothalamic mitochondrial dysfunction associated with anorexia in the anx/anx mouse.
Proc Natl Acad Sci U S A. 2011 Nov 1;108(44):18108-13 Epub 2011 Oct 24.
- Mulder J, Spence L, Tortoriello G, Dinieri JA, Uhlén M, Shui B, Kotlikoff MI, Yanagawa Y, Aujard F, Hökfelt T, Hurd YL, Harkany T.
Secretagonin is a Ca²⁺ binding protein identifying prospective extended amygdala neurons in the developing mammalian telencephalon.
Eur J Neurosci. 2010 Jun;31(12):2166-77 Epub 2010 Jun 7.
- Mulder J, Zilberter M, Spence L, Tortoriello G, Uhlén M, Yanagawa Y, Aujard F, Hökfelt T, Harkany T.
Secretagonin is a Ca²⁺ binding protein specifying subpopulations of telencephalic neurons.
Proc Natl Acad Sci U S A. 2009 Dec 29;106(52):22492-7 Epub 2009 Dec 16.
- Shi TJ, Xiang Q, Zhang MD, Tortoriello G, Hammarberg H, Mulder J, Fried K, Wagner L, Josephson A, Uhlén M, Harkany T, Hökfelt T.
Secretagogenin is expressed in sensory CGRP neurons and in spinal cord of mouse and complements other calcium-binding proteins, with a note on rat and human.
Mol Pain 2012 Oct 29;8:80.
- Zhang MD, Tortoriello G, Hsueh B, Tomer R, Ye L, Mitsios N, Borgius L, Grant G, Kiehn O, Watanabe M, Uhlén M, Mulder J, Deisseroth K, Harkany T, Hökfelt TG.
Neuronal calcium-binding proteins 1/2 localize to dorsal root ganglia and excitatory spinal neurons and are regulated by nerve injury.
Proc Natl Acad Sci U S A 2014 Mar 25;111(12):E1149-58.

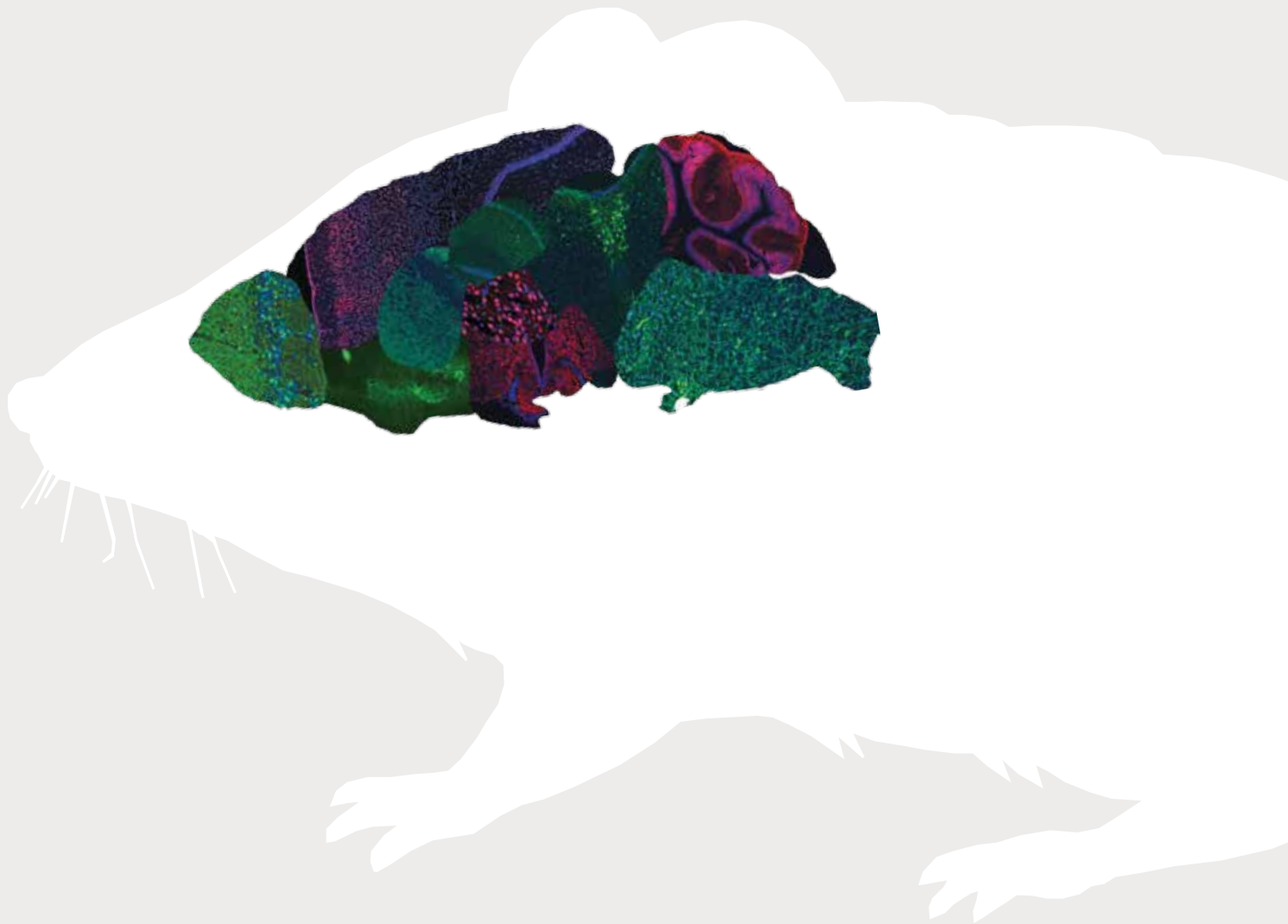


Dr. Jan Mulder
SciLifeLab Stockholm, Sweden

Dr. Mulder's group performs antibody based profiling of proteins in the human and rodent nervous system using biochemical and immunofluorescence techniques in combination with automated microscopy. The aim is to quantify and visualize regional, cellular and subcellular distribution of proteins in the developing, healthy and diseased nervous system.

In collaboration with the Human Protein Atlas (HPA) project, utilizing the unique antibody resource created within the project, they aim to 1) investigate protein distribution in a large portion of the nervous system using the smaller rodent brain and 2) identify changes in protein expression and distribution in the human brain affected by neurodegenerative disorders.

Many of the images within this catalog are from the work by Mulder *et al* as well as the list of Antibodies on the HPA Mouse Brain Atlas.



atlasantibodies.com

Our website provides you with easy access to all characterization data, and online ordering via our web shop. You can also send your order to order@atlasantibodies.com.

Or send an e-mail to support@atlasantibodies.com to discuss any matters regarding use of antibodies. **You'll find we're Totally Human.**